catalysts

MDPI

Review

Research Progress of Carbon Deposition on Ni-Based Catalyst for CO_2-CH_4 Reforming

Yuan Ren [1,†], Ya-Ya Ma [1,2,†], Wen-Long Mo [1,*], Jing Guo [3,*], Qing Liu [4], Xing Fan [4] and Shu-Pei Zhang [5]

[1] State Key Laboratory of Chemistry and Utilization of Carbon-Based Energy Resources and Key Laboratory of Coal Clean Conversion & Chemical Engineering Process (Xinjiang Uyghur Autonomous Region), School of Chemical Engineering and Technology, Xinjiang University, Urumqi 830046, China
[2] Qingdao Institute of Bioenergy and Bioprocess Technology, Chinese Academy of Sciences, Qingdao 266101, China
[3] School of Chemistry and Chemical Engineering, Ningxia Normal University, Guyuan 756000, China
[4] College of Chemical and Biological Engineering, Shandong University of Science and Technology, Qingdao 266590, China
[5] Xinjiang Yihua Chemical Industry Co., Ltd., Changji 831700, China
* Correspondence: mowenlong@xju.edu.cn (W.-L.M.); guojingsn@163.com (J.G.)
† These authors contributed equally to this work.

Abstract: As we all know, the massive emission of carbon dioxide has become a huge ecological and environmental problem. The extensive exploration, exploitation, transportation, storage, and use of natural gas resources will result in the emittance of a large amount of the greenhouse gas CH_4. Therefore, the treatment and utilization of the main greenhouse gases, CO_2 and CH_4, are extremely urgent. The CH_4 + CO_2 reaction is usually called the dry methane reforming reaction (CRM/DRM), which can realize the direct conversion and utilization of CH_4 and CO_2, and it is of great significance for carbon emission reduction and the resource utilization of CO_2-rich natural gas. In order to improve the activity, selectivity, and stability of the CO_2-CH_4 reforming catalyst, the highly active and relatively cheap metal Ni is usually used as the active component of the catalyst. In the CO_2-CH_4 reforming process, the widely studied Ni-based catalysts are prone to inactivation due to carbon deposition, which limits their large-scale industrial application. Due to the limitation of thermodynamic equilibrium, the CRM reaction needs to obtain high conversion and selectivity at a high temperature. Therefore, how to improve the anti-carbon deposition ability of the Ni-based catalyst, how to improve its stability, and how to eliminate carbon deposition are the main difficulties faced at present.

Keywords: CO_2-CH_4 reforming; Ni-based catalyst; carbon deposition

Citation: Ren, Y.; Ma, Y.-Y.; Mo, W.-L.; Guo, J.; Liu, Q.; Fan, X.; Zhang, S.-P. Research Progress of Carbon Deposition on Ni-Based Catalyst for CO_2-CH_4 Reforming. *Catalysts* **2023**, *13*, 647. https://doi.org/10.3390/catal13040647

Academic Editor: Avelina García-García

Received: 22 February 2023
Revised: 11 March 2023
Accepted: 20 March 2023
Published: 23 March 2023

1. Introduction

With the increasing use of fossil resources, such as coal, oil, and natural gas, the global CO_2 emissions will continue to rise. In recent years, some countries have been using renewable energy; however, this trend has not been enough to prevent the climate change, polar ice sheet melting, and hurricane intensification caused by the increase in CO_2 emissions. The massive emission of CO_2 not only accelerates the deterioration of the greenhouse effect but also wastes valuable carbon resources. Therefore, CO_2 reduction and resource utilization have become the most noticeable research issues. According to the proportions of different greenhouse gases in the total greenhouse gas emissions calculated by CO_2 equivalent, CH_4 accounts for 16% and is therefore the second villain of the greenhouse effect. Although the emission of CH_4 is far less than that of CO_2, its potential to produce a greenhouse effect is about 20 times more than that of CO_2. Therefore, how to convert the above two greenhouse gases into useful chemicals or chemical raw materials has attracted the great attention of governments and scientists around the world [1–3].

As early as 1928, Fischer and Tropsch discovered the carbon dioxide reforming of methane reaction, that is, $CO_2 + CH_4 = 2CO + 2H_2$ (carbon dioxide reforming of methane, CRM, ΔH = 247 kJ/mol), also known as methane dry reforming. CRM can produce synthesis gas; it is a strongly endothermic reaction, and the synthesis gas obtained has a low H_2/CO ratio, which is more suitable for the subsequent Fischer–Tropsch synthesis reaction [4]. The ratio of H_2/CO in the CRM product is about 1, and it can also be used in chemical reactions such as carbonyl synthesis and hydrocarbon production and to produce clean liquid fuels and high-value chemicals [5,6]. Hence, this reaction can also utilize CO_2 and CH_4, which are two main greenhouse gases; therefore, it has significant industrial value and ecological and environmental significance. The research on this reaction has been further developed, particularly in the past 30 years [7].

CRM and steam reforming of methane (SRM) are catalytic reactions at a high temperature (about 800 °C). The ΔH of CRM = 247 kJ/mol, which is greater than that of SRM (206 kJ/mol), indicating that both CRM and SRM are strongly endothermic reactions, and the endothermic capacity of CRM is nearly 20% higher than that of SRM. Therefore, the reverse reaction of CRM can theoretically release up to 247 kJ/mol of energy. Therefore, the reaction can be used as a good chemical energy transmission system (CETS) to store energy. On the other hand, CRM can be realized through fossil fuels (such as coal, petroleum, etc.), light energy, or nuclear energy, and the above energy can be stored in the product (synthesis gas); then, the synthesis gas can be transported to the place where it is needed for a reverse reaction to release energy.

Over a long period of time, researchers have conducted many studies on the selection and optimization of CRM catalysts, and have achieved fruitful results, making the research on this reaction increasingly broad and deep. Without loss of generality, the relationship between the chemical reaction itself, the type of active component and carrier, the modification of additives, the carbon deposition, and the catalyst performance have been consistently discussed by many researchers. As far as the CRM process is concerned, the main side reaction is the reverse water gas shift reaction ($CO_2 + H_2 = CO + H_2O$, reverse water gas shift reaction, RWGS), which consumes the H_2 ($CH_4 = C + 2H_2$) generated by CH_4 cracking and generates a large amount of CO, which can cause carbon deposition on the catalyst through another side reaction—the CO disproportionation reaction ($2CO = C + CO_2$) [8,9]. Thus, the proportion of CO_2 can be increased from the perspective of chemical equilibrium to inhibit the formation of carbon deposition (that is, the carbon elimination reaction, $C + CO_2 = 2CO$). Thermodynamic calculation showed that the RWGS reaction can be inhibited or avoided at temperatures above 820 °C, but this needs a lot of energy [10]. Therefore, how to optimize the catalyst structure, match the process conditions, and selectively control the degree of carbon deposition, the reverse water gas shift reaction, carbon elimination, and other chemical reactions involving carbon is of great significance in improving the activity of the CO_2-CH_4 reforming catalyst, inhibiting catalyst deactivation, and extending the service life of the catalyst.

Pakhare et al. [11] introduced DRM literature on a catalyst based on Rh, Ru, Pt, and Pd metals. This includes the effect of these noble metals on the kinetics, mechanism, and deactivation of these catalysts. The inert support catalysts are more prone to deactivation due to carbon deposition than the acidic or basic supports.

At present, the widely used CO_2-CH_4 reforming catalyst is still dominated bythe non-noble metal catalyst, especially the Ni-based catalyst. Its activity is equivalent to that of the noble metal, but it is very easily inactivated due to carbon deposition. Therefore, the development of the Ni-based catalyst with high carbon deposition resistance is the key to realizing the industrialization of CO_2-CH_4 reforming. A large number of studies have shown that carbon deposition in the hydrocarbon conversion process is mainly affected by such factors as the acid–base property of the carrier, the dispersion of the active component, and the interaction between the carrier and the active metal [12–16]. The acid sites on the catalyst surface are not conducive to the adsorption of CO_2, resulting in the carbon deposition rate on the catalyst surface being much higher than the carbon

elimination. Conversely, the surface basic sites can inhibit the carbon deposition caused by CO disproportionation to a certain extent, thereby improving the stability of the catalyst. It was found that when the particle size of the active component was less than 10 nm, the catalyst could present a high anti-coking performance [14]. In addition, strong metal-support interaction is also beneficial in improving the anti-carbon deposition performance of the catalyst [15,16].

In this paper, the thermodynamics, kinetics, and reaction mechanism of the CO_2-CH_4 reforming reaction are reviewed. Because Ni-based catalysts exhibit high activity but have the problem of the easy deactivation of carbon deposition, this paper further summarizes the research situation regarding carbon deposition on Ni-based catalysts, including the types of carbon deposition, the amount of carbon deposition, and the elimination of carbon deposition. As to how to improve the anti-carbon deposition ability of the Ni-based catalyst and how to eliminate carbon deposition, this paper focuses on two aspects: one is the resistance of carbon deposition from the perspective of catalyst optimization; the other is the elimination of carbon deposition from the perspective of process condition matching. Finally, how to improve the carbon deposition resistance of Ni-based CRM catalyst is prospected.

2. Thermodynamics of CO_2-CH_4 Reforming

CO_2-CH_4 reforming mainly includes the following reactions:

$$CH_4 + CO_2 = 2H_2 + 2CO,\ \Delta H\ (298\ K) = 247\ kJ/mol, \quad (1)$$

$$H_2 + CO_2 = H_2O + CO,\ \Delta H\ (298\ K) = 41\ kJ/mol, \quad (2)$$

$$2CO = CO_2 + C,\ \Delta H\ (298\ K) = -172\ kJ/mol, \quad (3)$$

$$CH_4 = C + 2H_2,\ \Delta H\ (298\ K) = 75\ kJ/mol, \quad (4)$$

$$CO + H_2 = C + H_2O,\ \Delta H\ (298\ K) = -131\ kJ/mol, \quad (5)$$

Zhang et al. [17] obtained the thermodynamic equilibrium constants of the above reactions as a function of temperature through thermodynamic calculations, as shown in Figure 1.

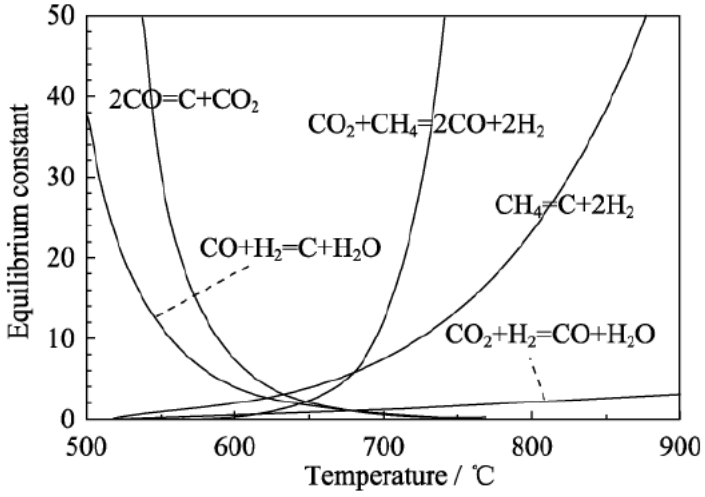

Figure 1. Equilibrium constants of reactions as a function of temperature during DRM [17].

As both methane and carbon dioxide are very stable, CRM is an extremely strong endothermic reaction. Meanwhile, the RWGS reaction is an important side reaction in the CRM process which reduces the H_2/CO ratio in the product [18,19]. In the CRM reaction process, high temperature (>1000 K) and low pressure (~1 atm) are usually required to obtain the efficient conversion of methane and carbon dioxide to syngas. At a higher

pressure, it can promote the RWGS reaction and reduce the H_2/CO ratio. Therefore, the ratio of carbon dioxide and methane in the feed gas has a great influence on the H_2/CO ratio. Many experiments showed that the ideal H_2/CO ratio of 1 can be achieved when the CO_2/CH_4 ratio is about 1. With the increase in the CO_2/CH_4 ratio, the H_2/CO ratio decreases. This trend is more obvious at higher pressures (10 atm).

In addition to RWGS, there are two other side reactions, methane decomposition and CO disproportionation, which also occur in the CRM process [11]. These two reactions lead to the formation of carbon deposition, which leads to the deactivation of the catalyst. In order to study the formation of the carbon deposition, Lu et al. [19] calculated the limit temperatures of the two side reactions (where the Gibbs free energy change is zero). The CO_2-CH_4 reaction can be accompanied by methane cracking at above 640 °C, while the reverse water gas shift reaction starts at above 820 °C, without CO disproportionation ($2CO = C + CO_2$, the Boudouard reaction). In the range of 557–700 °C, carbon is mainly formed by methane cracking or the Boudouard reaction. Under the pressure of 0.01–0.1 atm, the feed ratio of $CO_2/CH_4 = 1$ can reach the equilibrium conversion rate. At a fixed temperature, the rate at a low pressure is always higher than that at a high pressure. Under the pressure of 0.01 atm, the rate reached 90% at 550 °C, and did not reach 90% until 700 °C at 0.1 atm. There is an upper temperature limit for carbon deposition, and the temperature increases with the increase in reaction pressure and the decrease in the CO_2/CH_4 ratio. Therefore, the formation of carbon deposition at a certain temperature can be inhibited by reducing the reaction pressure and increasing the proportion of carbon dioxide in the feed gas.

The main reactions of carbon deposition are methane decomposition and the carbon monoxide disproportionation reaction. Severe carbon deposition will lead to blockage or even deactivation of the catalyst bed. According to thermodynamic analysis, the carbon monoxide disproportionation reaction is a strongly exothermic reaction, which mainly occurs in a relatively low temperature range (<650 °C), and methane cracking reaction is a strongly endothermic reaction, which mainly occurs in a relatively high temperature range. Therefore, low temperature and high pressure are beneficial to carbon monoxide disproportionation, and high temperature and low pressure are beneficial to methane cracking, and the main reaction temperature is in the range of 557–700 °C. When the temperature is higher than 600 °C, the amount of carbon deposition will increase rapidly. However, with the increase in reaction temperature, the disproportionation reaction of carbon monoxide will be inhibited, and methane cracking will become the main reaction of the carbon deposition [11,20,21]. However, a high reaction temperature often leads to both the sintering of the active metal and carbon deposition on the catalyst. Sometimes, the fibrous carbon formed during the reaction process has a high mechanical strength, which will damage the catalyst and lead to rapid deactivation of the catalyst [18,19,22].

Adding O_2 to CRM system can remove the carbon deposition formed to promote the regeneration of the catalyst, and the heat released from the reaction can also accelerate the decomposition of the methane. For periodic operation, the addition of oxygen (CO_2/O_2 ratio of 7/3) during the regeneration process at 750 °C significantly improved the stability and activity of the catalyst. During the stability experiment, the catalytic performance of the $Ni/SiO_2{\cdot}MgO$ catalyst for CRM in the presence of O_2 increased with the increase in O_2 content and reaction temperature [23]. In addition, the introduction of another auxiliary means, such as light and plasma treatment, can break the energy barrier of the reaction and improve the conversion rate of the reactants. Some researchers used Au as the plasma promoter for the first time to improve the reforming performance of noble metal-based catalysts. The results showed that visible light irradiation could significantly improve the reforming activity of the Rh-Au/SBA-15 catalyst. The maximum CO_2 conversion rate under light conditions is 1.7 times higher than that under dark conditions. The test at 400 °C showed that the CO_2 conversion rate under light conditions was 2.4 times higher than that under dark conditions. Kinetic measurement showed that the activation energy was reduced by 30% under light conditions [24].

3. Kinetics of CO_2-CH_4 Reforming (Reaction Mechanism)

With the development of research technology at the micro-level, the perspective of the theoretical research has gradually shifted from thermodynamics to kinetics. The view on the adsorption and dissociation of reactants and products provides an ideal explanation for the kinetics of the CRM reaction.

Presently, the focus of the research on CO_2-CH_4 reforming has two aspects. On the one hand, it is necessary to find new catalysts and additives to improve the catalyst activity and carbon deposition resistance. On the other hand, it is necessary to study the reaction mechanism in detail by the kinetic method, with the aim of deeply understanding the reforming reaction and designing a new catalyst according to the mechanism. Kinetic study is one of the best methods to reveal the intrinsic activity of the used catalyst. Due to the high activity and low price of Ni in CO_2-CH_4 reforming, the study of Ni kinetics has attracted more and more attention. Most studies have focused on exploring the rate-determining step in the CO_2-CH_4 reforming process. Discussing the rate-determining step of the reaction can lead to further understanding of the catalytic reaction mechanism and the design and improvement of the catalyst and reaction conditions. It was found that the kinetic process of CO_2-CH_4 reforming mainly includes the adsorption and dissociation of the reactants, CH_4 and CO_2, as well as the formation and desorption of the products, H_2 and CO. In order to correctly understand the kinetics and reaction mechanism of the reaction, we should understand the adsorption, desorption, and reaction properties of the reactants and products on the catalyst.

CRM reaction is a complex process. The mechanism of CRM varies greatly according to the difficulty in forming reaction intermediates in different catalyst systems and reaction conditions [25]. Many studies have shown that the key step of CRM is the adsorption and dissociation of CH_4 on the catalyst surface.

The reaction mechanism of CO_2-CH_4 reforming is closely related to the type and composition of the catalyst. At present, there is no uniform conclusion on the reaction mechanism of CO_2-CH_4 dioxide reforming. Many researchers have explored the mechanisms of different catalysts.

Bodrov et al. [26] first proposed the CO_2-CH_4 reforming reaction principle on a Ni-based catalyst, including the following basic steps:

$$CH_4 + * \rightarrow CH_2* + H_2, \quad (6)$$

$$CO_2 + * \longleftrightarrow CO + O*, \quad (7)$$

$$O* + H_2 \longleftrightarrow H_2O + *, \quad (8)$$

$$CH_2* + H_2O \longleftrightarrow CO* + 2H_2, \quad (9)$$

$$CO* \longleftrightarrow CO + *, \quad (10)$$

In the above formula, "*" represents the active site, (6) represents an irreversible slow reaction, and the other steps are reversible reactions.

Later, Hansen et al. [27] improved the above mechanism and proposed that the dissociation of CH_4 on Ni/MgO can be divided into two steps:

$$CH_4 + * \rightarrow CH_3* + H*, \quad (11)$$

$$CH_3* + (3 - x)* \rightarrow CH_x* + (3 - x)H*, \quad (12)$$

Osaki et al. [28] analyzed the surface pulse reaction rate of a Ni/MgO catalyst and found that the adsorption and dissociation of CH_4 can directly generate gaseous H_2, namely

$$CH_4 + * \rightarrow CH_x* + (4 - x)/2H_2*, \quad (13)$$

It was experimentally concluded that the dissociation of CH_4 was the rate-determining step of the CO_2-CH_4 reforming reaction.

For Ni and Pt-based catalysts, Bradford et al. [29] believed that CH_4 first dissociated into CH_x* and H_2, while CO_2 dissociated under the action of H* to form CO* and OH*; then, CH_x* reacted with OH* to form CH_xO*, and finally, CH_xO* decomposed into CO and H_2.

Wei et al. [30] studied the kinetics of the CO_2-CH_4 reaction on a Ni/MgO catalyst by using carbon dioxide and methane isotopes. They observed an obvious isotope effect of CH_4 dissociation and speculated that CH_4 dissociation was the rate-determining step of the reforming reaction. In the field of theoretical research, Wang et al. [31] used the DFT (density functional theory) method to study the principle of the CO_2-CH_4 reaction on the surface of perfect Ni(111). The calculation results showed that the principle of CO_2-CH_4 reforming is:

1. CO_2 decomposes to generate O and CO, while CH_4 gradually cleaves H on the surface to generate CH and H_2;
2. CH is oxidized to obtain CHO;
3. The main product CO is obtained by the dissociation reaction of CHO;
4. H_2 and CO are desorbed from Ni(111) to form free H_2 and CO.

Although the activation mechanisms of different catalytic systems are quite different, the existing research results show that the dehydrogenation cracking of CH_4 on the metal surface is a common and critical process. That is, CH_4 is decomposed into surface CH_x (x = 1–3) and H ($CH_4 \rightarrow CH_3 \rightarrow CH_2 \rightarrow CH$). On the other hand, the adsorption and activation mechanism of CO_2 is very important for the decarbonization process, because it not only generates the key product CO, but also provides a surface oxygen species for CH_4 reforming, which is the core intermediate for the elimination of carbon deposition. CO_2 activation consists of two steps: the first step is CO_2 chemical adsorption and the formation of an anionic $CO_2^{\delta-}$ precursor on the surface [32,33]; in the second step, the $CO_2^{\delta-}$ precursor is dissociated into surface adsorbed CO and O species. Therefore, CO_2 is the only source of the oxygen atom in the reaction gas and is the supplier of active oxygen species on the catalyst surface [34–38]. In addition, the activation path of CO_2 varies with the acidity and alkalinity of the support, which has a certain effect on the anti-carbon deposition performance of a Ni-based catalyst. Generally, at the interface between the active metal and the support, the acidic support can promote the dissociation of CH_4, but the stronger the acidity, the easier it is to produce carbon deposition [39].

It is known that increasing the adsorbed oxygen species over the catalyst surface is really effective in promoting the catalytic activity and restraining the side reaction (RWGS). Simultaneously, the adsorbed oxygen species are effective in suppressing/removing the deposited carbon, thereby alleviating catalyst deactivation [40].

The higher CO_2 activity enhanced the oxidation rate of the surface carbon generated from the side reactions, thereby resulting in a higher reforming rate and in the inhibition of the coke formation, especially the detrimental graphitic encapsulating carbon on an active nickel surface [41].

Based on the combined results of catalytic testing and characterization, Ni/$Ce_{0.9}Eu_{0.1}O_{1.95}$-HT can accelerate the rate of CO_2 activation and promote the conversion of CH_4 into CO instead of into coke deposition, leading to a relatively good performance for the DRM reaction [42].

Burghaus [43] clarified the correlation between CO_2 adsorption kinetics and the surface structure characteristics of various metals and oxides, including metals (Cu, Cr), metal oxides (ZnO, TiO_2, CaO), model catalysts (Cu/ZnO, Zn/Cu), and nano-catalysts. The binding energy of CO_2 and metal oxides is generally greater than that of metals. When CO_2 chemisorption occurs on CaO, the C atom combines with the O site of CaO, and the surface carbonate formed is very stable. Its decomposition and desorption temperature is as high as 1100 K.

Pan et al. [44] used DFT calculation and found that the adsorption and activation of a 3D transition metal dimer (M_2/γ-Al_2O_3, M = Sc, Ti, V, Cr, Mn, Fe, Co, Ni, Cu) supported by γ-Al_2O_3 were consistent with the experimental results reported in many of the studies.

CO_2 adsorbed on M_2/γ-Al_2O_3, a negatively charged species is formed, forming a metal dimer; γ-Al_2O_3 supports could provide electrons to the adsorbed CO_2 to activate it, and the most favorable adsorption position was at the interface between the metal dimer and the support; so, the highly dispersed metal particles showed good activity. In addition, the hydroxyl group on the surface of the carrier reduces the amount of charge transferred from the metal dimer to the CO_2 and weakened the chemical adsorption of CO_2.

The addition of La_2O_3 to the Ni/γ-Al_2O_3 catalyst could inhibit the carbon deposition in CO_2-CH_4 reforming. Some researchers have found that in the CO_2-CH_4 reaction, La_2O_3 interacts with CO_2 on the Ni/La_2O_3 catalyst to generate $La_2O_2CO_3$ [45], and $La_2O_2CO_3$ decomposes CO and provides oxygen species, and the oxygen species can react with carbon species accumulated after the dissociation of CH_4 on Ni grains to generate CO, thus achieving the effect of inhibiting carbon deposition.

4. Carbon Deposition and Elimination on Ni-Based Catalyst

The Ni-based catalyst is widely used in industrial processes because of its high activity, good stability, and low cost, but the biggest problem is that the catalysts are easily inactivated. There are three main ways that deactivation occurs: carbon deposition, sintering, and poisoning. Among them, the most important factor causing catalyst inactivation in the carbon-related reaction process was carbon deposition. Hence, the reaction mechanism of carbon deposition and the inhibition of carbon deposition need to be further studied. The several existing inhibition methods can be divided into two types: one involves the resistance of carbon deposition from the perspective of catalyst optimization, and the other involves the elimination of carbon deposition from the perspective of process condition matching.

4.1. Formation and Type of Carbon Deposition

The deactivation of the Ni-based catalyst is mainly due to carbon deposition on the catalyst surface. The raw materials for the CO_2-CH_4 reforming reaction are all carbon-containing gases. Methane cracking ($CH_4 = C + 2H_2$) and carbon monoxide disproportionation ($2CO = C + CO_2$) will inevitably form carbon on the catalyst surface [11].

According to existing studies, the types of carbon deposition can be divided into amorphous carbon, polymerized carbon, carbon nanotubes, graphitized carbon, and filamentous carbon [46]. Amorphous carbon is composed of carbon atoms adsorbed on the metal active center; these atoms have high reactivity and can be removed by an oxidation reaction ($C + O_2 = CO_2$) at about 200 °C. Polymerized carbon composed of partially hydrogenated carbon-carbon chains has low reactivity, but it is still a kind of carbon species that can be oxidized and eliminated under mild conditions or eliminated under appropriate process conditions (such as excessive CO_2). Graphitized carbon is a ring structure composed of six carbon atoms and needs higher a reaction temperature to be oxidized and eliminated. It belongs to inert carbon deposition. Filamentous carbon and carbon nanotubes can block the pores of the catalyst and gradually reduce its activity until it is completely deactivated [7,47,48].

Mo et al. [49] studied the effect of reaction time on carbon deposition on a Ni-Al_2O_3 catalyst. Figure 2 shows the TPH spectra of samples after a reforming reaction at different times. According to the report [50], 200–350 °C is the first type of hydrogenation peak, which belongs to the amorphous α type of carbon species, which is the active intermediate of the decarbonization reaction ($CO_2 + C = 2CO$) and is also the desired type of carbon deposition for a carbon-related reaction. It is easy for this type of carbon to be converted into a slightly less active carbon at a high-temperature β type of carbon species; 350–500 °C is the second type of hydrogenation peak, which belongs to the β_1 type carbon species, which do not form a strong interaction with the carrier and are easy to deposit in the catalyst pore, or they enter the catalyst lattice to form carbon nanotubes or filamentous carbon; they have decarbonization reaction activity at higher temperatures but easily become inert when aggregated for a long time at high-temperature γ carbon species; 500–700 °C is the third

type of hydrogenation peak, belonging to the γ type of carbon species, such as graphite carbon, whose activity is lower than α carbon and β carbon and is an important reason for the irreversible deactivation of the catalyst due to carbon deposition. The literature also showed that [51], after the CRM reaction occurred on the surface of the Ni-CaO-ZrO_2 catalyst for 1 h, the temperature-programmed hydrogenation reaction characterization (TPH) found that the coking hydrogenation peak at about 800 °C was attributable to β_2 types of carbon species, namely the fourth type of hydrogenation peak. It can be seen from Figure 2 that in the process of the CO_2-CH_4 reforming reaction on the Ni-Al_2O_3 catalyst, the surface hydrogenation peaks of the carbon species generated are all at 200–500 °C, that is, the amorphous carbon C_α and filamentous carbon $C_{\beta 1}$ type exists [52,53]. However, no obvious hydrogenation peak was found at about 600 and 800 °C. Therefore, it can be considered that in the range of 10 h, the CO_2-CH_4 reforming reaction almost did not form the C_γ and $C_{\beta 2}$ types of carbon species.

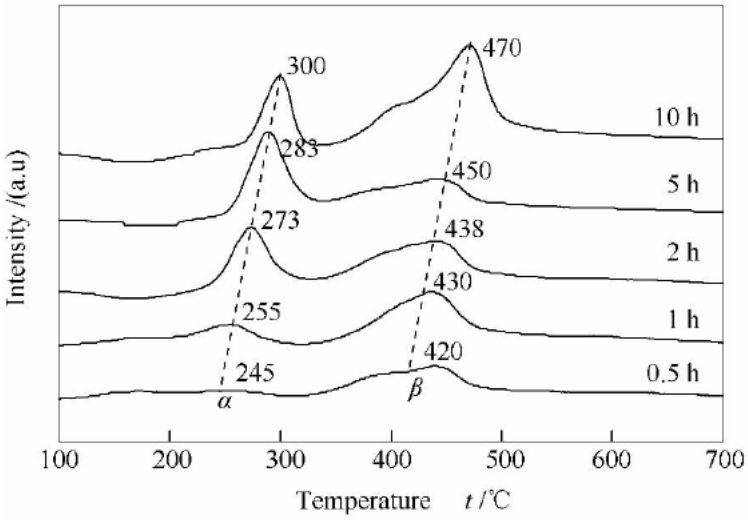

Figure 2. TPH profiles of various spent Ni-Al_2O_3 catalysts after carrying out the CO_2-CH_4 reforming reaction for different times [49].

According to the degree of difficulty of carbon elimination under the conditions of the reforming reaction, the above carbon deposition can be classified as active carbon deposition (amorphous carbon), transitional carbon deposition (polymeric carbon, carbon nanotubes, and filamentous carbon), and inactive carbon deposition (graphitized carbon).

Mo et al. [49] observed the carbon deposition on the catalyst surface at different reaction times and found that the fibrous carbon deposition began to accumulate after 2 h of reaction, and after 5 h, it was observed that there were many fibrous or rod-shaped morphologies with larger diameters. With the extension of reaction time, the amount of fibrous carbon deposition increased significantly, while the diameter of the carbon fibers decreased significantly, which is probably because of the occurrence of a carbon elimination reaction ($C + CO_2 = 2CO$) in CO_2-CH_4 reforming (Figure 3). The results also showed that each sample had two hydrogenation peaks, one low-temperature hydrogenation peak and one high-temperature hydrogenation peak, corresponding to two types of carbon deposition species [49]. With the increase in reaction temperature, the high-temperature hydrogenation peak of the carbon deposition moves to a high temperature. The reaction temperature increased from 650 °C to 850 °C, and the peak temperature of the high-temperature hydrogenation peak increased from 425 °C to 455 °C, which may be due to the fact that filamentous carbon is easily converted into graphite carbon at high temperatures, and the hydrogenation reaction needs to be carried out at a higher temperature [54].

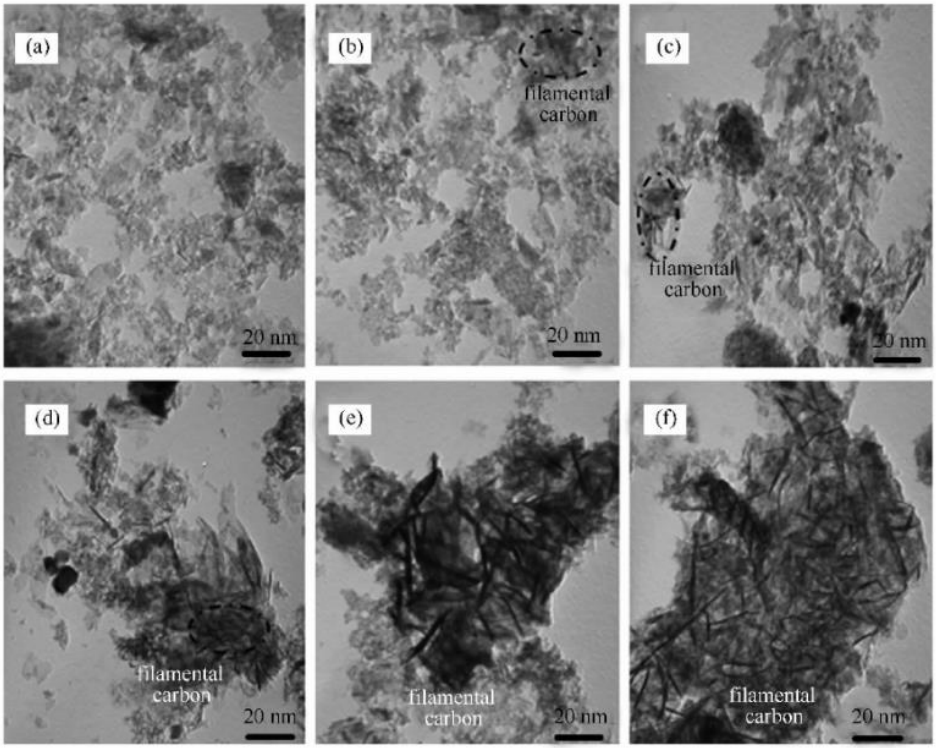

Figure 3. TEM photos of different Ni-Al_2O_3 catalysts after CO_2-CH_4 reforming reaction for different times [49]. (**a**–**f**) Fresh catalyst and catalyst after reaction for 0.5 h, 1 h, 2 h, 5 h, and 10 h, respectively.

Figure 4 showed the morphological characteristics of carbon on the catalyst surface after the reforming reaction. It can be seen from the figure that a large amount of filamentous carbon is formed on the catalyst surface and is even covering the catalyst surface in a large range. It can be speculated that if the carbon deposition continues, it will completely cover the catalyst surface and cause catalyst deactivation [46].

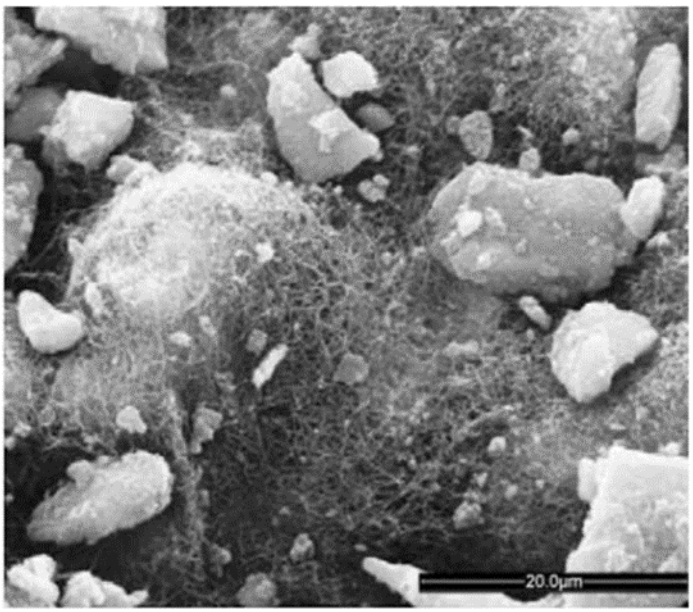

Figure 4. SEM of CO_2-CH_4 reforming reaction after 20 h [46].

4.2. Resistance and Elimination of Carbon Deposition

In CO_2-CH_4 reforming, the carbon deposition rate usually depends on its formation rate and elimination rate. When the elimination rate of carbon deposition is higher than the

formation, the carbon deposition can be inhibited [55]. According to the cause of carbon deposition in the CO_2-CH_4 reaction, the carbon deposition can be suppressed by two aspects: catalyst modification and process conditions optimization.

In the process of CO_2-CH_4 reforming, carbon deposition mainly comes from methane cracking and carbon monoxide disproportionation. The dehydrogenation of CH_4 on the metal surface generates carbon species CH_x (x = 0–3, $CH_4 \rightarrow C + 2H_2$), which do not react with the surface oxygen species generated by the timely adsorption and dissociation of CO_2 to generate carbon species of CO ($C + CO_2 \rightarrow 2CO$), and the carbon species may accumulate on the metal surface, causing carbon deposition. As the carbon dioxide content in the reactant gas increases, the adsorption rate of methane and its subsequent dissociation rate (i.e., the cracking of methane) decrease. At the same time, the oxidation rate of carbon species on the catalyst surface increases. Therefore, the amount of carbon deposited on the active site is reduced, which can significantly improve the stability of the Ni-based catalyst. In an atmosphere with sufficient CO_2, during a long catalytic process, carbon will migrate and accumulate in the center of the Ni crystal, forming a hollow fiber type structure from bottom to top. The process of carbon deposition and carbon elimination on a Ni/CeO_2 catalyst is shown in Figure 5 [56].

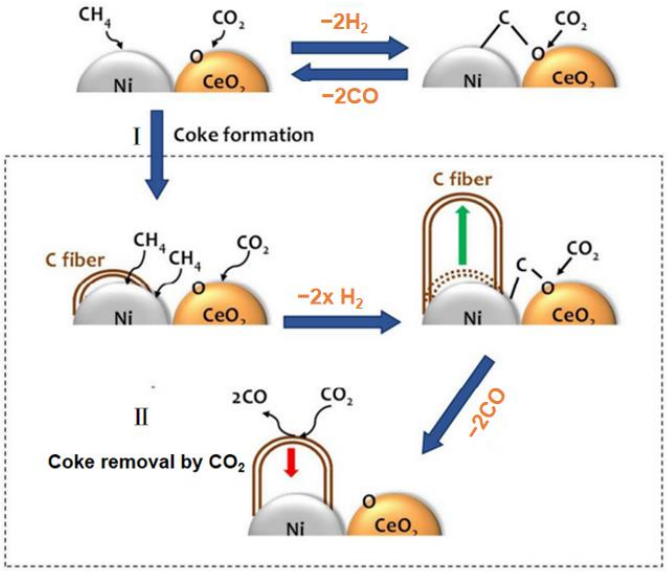

Figure 5. Carbon deposition and decarbonization on Ni/CeO_2 catalyst [56].

Kuijpers [57] found the size sensitivity of CH_4 activation in the study of Ni-based catalysts, that is, CH_4 preferentially dissociates on smaller Ni grains. Osaki et al. [28,58] reported the x value of CH_x species on different catalysts: Ni/MgO = 2.7, Ni/ZnO = 2.5, Ni/Al_2O_3 = 2.4, Ni/TiO_2 = 1.9, Ni/SiO_2 = 1.0, and Co/Al_2O_3 = 0.75. It can be seen that for the same metal, the x value of basic carrier is higher, that is, the degree of CH_4 dissociation increases with the increase in carrier acidity. On the other hand, the activation of the C-H bond requires electrons from the surface of the Ni; so, the electronic environment around the Ni is also extremely important [59]. For example, the strong metal-support interaction will significantly affect the activity of Ni to dissociate CH_4 [60,61].

Horiuchi et al. [7] believe that alkaline metal oxides can enhance the adsorption capacity of CO_2 and generate more active oxygen atoms (O_{ad}); O_{ad} can effectively prevent the adsorption of $CH_{x,ad}$ on the active center of Ni metal through the reaction of $CH_{x,ad} + O_{ad} \rightarrow CO + H_2$, thus avoiding the surface carbon deposition caused by the cracking of $CH_{x,ad}$. Therefore, adding additives such as alkali or alkaline oxide can enhance the basicity of the carrier surface and the ability to absorb CO_2, change the electronic density of the metal active center, effectively improve the catalytic activity of the catalyst, and inhibit the carbon deposition on the catalyst surface [62].

4.2.1. Resistance of Carbon Deposition from the Perspective of Catalyst

Effect of Ni Grain Size on the Deposition of Carbon

Studies have shown that high dispersion of active metal on the surface of the support can reduce the agglomeration size and effectively inhibit carbon deposition [11,63,64]. It has also been shown that only when the size of the active component is larger than a certain critical size (for example, ≥9 nm) can lead the carbon simple substance to form nuclei [7]. The small size and high dispersion of the active component can effectively inhibit the nucleation and growth of carbon whiskers. Therefore, by selecting the appropriate support, additive, and preparation method, the metal dispersion and particle size can be adjusted to effectively inhibit the occurrence of carbon deposition and improve the anti-carbon deposition performance [65]. In addition, the addition of an appropriate additive can also improve the surface alkalinity of the catalyst, strengthen the adsorption of CO_2, promote the elimination of deposited carbon species, and enhance the anti-carbon deposition performance of the catalyst.

XU et al. [66] prepared Ni/La_2O_3/γ-Al_2O_3 and Ni/La_2O_3/α-Al_2O_3 catalysts and found that when the size of the Ni particles was less than 15 nm, the carbon deposition was significantly reduced (Figure 6), which made the catalyst have higher catalytic activity and stability. CRNIVEC et al. [67] found that the catalyst surface with metal active particles less than 6 nm has excellent resistance to carbon deposition. LIU et al. [68] found that when nickel particles were less than 5 nm, they had an obvious inhibition effect on carbon deposition.

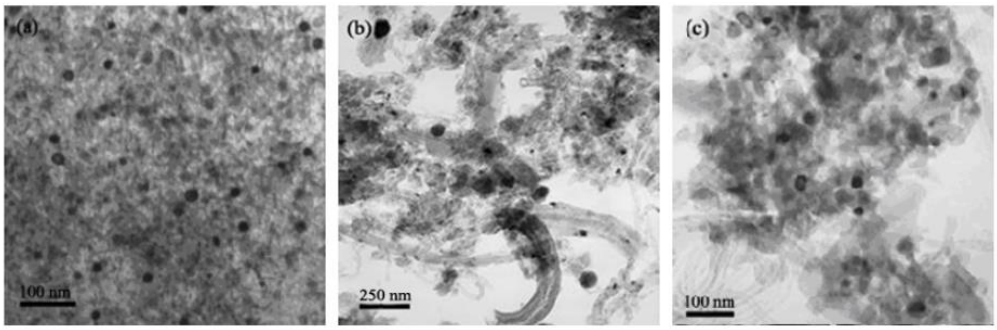

Figure 6. TEM images of catalyst after reaction [66]: (**a**) Ni/La_2O_3/γ-Al_2O_3; (**b**) Ni/La_2O_3/Al_2O_3; (**c**) Ni/La_2O_3/α-Al_2O_3.

Li et al. [69] analyzed the surface carbon on a Ni/MgO catalyst based on density functional theory and found that the size of the active component Ni had a great influence on the anti-carbon deposition performance of the catalyst. The three different sizes of active metals, Ni4, Ni8, and Ni12 were loaded on the surface of MgO, showing significant differences in catalytic activity and stability. Small size Ni4 can reduce the activation energy of the CH_4 dissociation adsorption, the CH dissociation, and the Coxidation, thus improving the CO_2-CH_4 reforming performance.

In their study, Mo et al. [70,71] found that after the reduction in the Ni-based catalyst based on $NiAl_2O_4$ spinel, the size of the Ni crystal was small and could effectively prevent the high-temperature sintering of the active component. By increasing the calcination temperature, the proportion of $NiAl_2O_4$ spinel (the active component precursor) in the catalyst was increased, and the size of the active component was effectively reduced; the stability of the catalyst was improved, and the amount of carbon deposited on the catalyst was obviously reduced. It was also found that there were two Ni precursors, crystalline NiO (calcinated at lower temperature (≤600 °C) and spinel $NiAl_2O_4$ (calcinated at higher temperature (≥700 °C), indicating that the calcination temperature significantly affected the interaction force between the metal and the support. The higher the calcination temperature, the stronger the force, and the more the spinel phase Ni species that formed. This type of Ni species gave a small size of active component after reduction, which could obtain higher CO_2 and CH_4 conversion and H_2 selectivity [72].

Inhibition of Carbon Deposition from the Stability of Ni Component

In general, researchers add some additives to the Ni-based catalyst to improve the dispersion and stability of the nickel, promoting the reforming reaction and inhibiting the formation of carbon deposition, which is a research hotspot in this reaction. The additives commonly used are mainly divided into two categories. The first type of additive is alkaline oxides, including MgO, CaO, K_2O, etc. [73,74]. It was found that the addition of alkaline oxides to a Ni-based catalyst can promote dispersion of the Ni and inhibit carbon deposition. On the other hand, the alkaline medium can improve the adsorption performance of CO_2 (weak acid gas). Some researchers [74] believed that the addition of alkali metals can inhibit carbon deposition and improve the activity and stability of the catalyst. Mo et al. [75] studied the effect of CaO on the structure, reforming performance, and carbon deposition of the Ni-Al_2O_3 catalyst. The results showed that the activity of Ni-Ca-4 was higher, with the conversion rate of CH_4 and CO_2 of 52.0% and 96.7%, respectively. The amount of carbon deposited on the catalyst was lower, and the type of the carbon was attributed to an amorphous one, presenting a good anti-carbon deposition performance.

Another kind of additive is rare earth oxides [73], such as CeO_2 and La_2O_3, which can achieve both high activity and stability for CO_2-CH_4 reforming. By adding rare earth oxide, the crystal phase, pore structure, and mechanical strength of the catalyst could be significantly changed, thereby improving the activity, stability, and selectivity of the catalyst. For example, the addition of La_2O_3 to the Ni/γ-Al_2O_3 catalyst could inhibit the carbon deposition in CO_2-CH_4 reforming. Some researchers found that in the CO_2-CH_4 reaction, La_2O_3 interacts with CO_2 on the Ni/La_2O_3 catalyst to generate $La_2O_2CO_3$ [52]; $La_2O_2CO_3$ decomposes CO and provides oxygen species, and the oxygen species can react with the carbon species accumulated after the dissociation of CH_4 on Ni grains to generate CO, thus achieving the effect of inhibiting carbon deposition. Other additives, such as metal Cr [76] and mixed oxide CeO_2-ZrO_2 [77,78], can also improve the activity and stability of the catalyst.

Mo et al. [70] prepared a series of La_2O_3-NiO-Al_2O_3 catalysts with different La loading to improve the performance of the Ni-based catalyst for CO_2-CH_4 reforming. The results showed that the precursor of the active component mainly exists in the form of $NiAl_2O_4$ spinel. The "confinement effect" of La_2O_3 on Ni grains can inhibit the sintering of the active component, prevent carbon deposition, and improve the reforming performance. Mo et al. [79] also prepared a Ni-Al_2O_3 catalyst with Ca, Co, and Ce as additives by the combustion method. The results showed that the activity order of the catalysts was followed by Co-Ni-Al_2O_3>Ca-Ni-Al_2O_3>Ni-Al_2O_3>Ce-Ni-Al_2O_3. Carbon deposition analysis showed that Ca-Ni-Al_2O_3 presented poor carbon deposition resistance, and a certain amount of graphitic carbon was generated on the catalyst. The dry reforming performance of Ni catalysts supported by different supports is shown in Table 1

Table 1. Catalytic performance of Ni-based catalysts with different supports.

Active Component	Support	Mass Fraction of Active Component /%	Temperature /°C	Time /h	SV /(mL·g^{-1}·h^{-1})	CH_4 Conversion Rate /%	CO_2 Conversion Rate /%	Carbon Deposition /%	Reference
$LaNiO_3$	SBA-15	10	700	60	36,000	78	73	4.47	[80]
$LaNiO_3$	MCM-41	10	700	60	36,000	75	71	4.83	[80]
$LaNiO_3$	SiO_2	10	700	60	36,000	68	64	5.67	[80]
Ni	MgO	20	750	2.3	168,000	46.13→34.3	51.4→37.6	2.648	[81]
Ni	Al_2O_3-T	10	700	5	24,000	80	90	——	[82]
Ni	Al_2O_3-S	10	700	5	24,000	68	79	——	[82]
Ni	Al_2O_3	10	700	5	24,000	72	75	——	[82]
Ni	γ-Al_2O_3-S	10	700	5	48,000	56.0→52.2	——	——	[83]
Ni	γ-Al_2O_3-P	10	700	5	48,000	52.2→39.3	——	——	[83]
Co-Ni	CeO_2	——	600	10	12,000	77	80	——	[84]
Ni	MgO-ZrO_2	10	700	60	16,000	84.7	86.5	20	[85]
Ni	ZrO_2-RC-100	5	700	7	42,000	67.4→46.5	68.4→58.2	66.3	[86]
Ni	ZrO_2-ELTN	5	700	7	42,000	42.3→31.9	52.3→43.9	25.2	[86]
Ni	ZrO_2-Z-3215	5	700	7	42,000	62.2→45.3	69.5→58.4	38.3	[86]
Ni	ZrO_2(MK)	5	700	7	42,000	51.2→36.3	56.7→46.4	46.9	[86]
Ni	ZrO_2-O_2	10	750	10	24,000	78→64	86→73	——	[87]
Ni	ZrO_2	5	750	36	24,000	83→78	——	——	[87]

Application of High-Activity Bimetallic Catalysts

The introduction of a second metal to obtain a bimetallic Ni-based catalyst is also considered to be an effective and practical strategy to improve the performance of the CRM catalyst. The synergistic effect between Ni and the second metal can significantly improve the activity and carbon deposition resistance of the Ni-based catalyst [17,88–91].

In order to discuss the synergistic effect and the basic principle for improving the performance of the used catalyst, the researchers prepared a series of bimetallic Ni-based CRM catalysts. The results showed that Ni-Pt [92], Ni-Co [93], and Ni-Cu [94] showed better activity and carbon deposition resistance. In general, bimetallic Ni-based CRM catalysts include Ni-noble metals (Pt, Ru, etc.) and Ni-transition metals (Co, Fe, and Cu) [95,96]. Ni-noble metal bimetallic catalysts have three advantages: the promotion of reduction, surface modification, and surface reconstruction. Noble metals usually contribute to the reduction in NiO crystal, thereby increasing the number of active sites [97–100]. In terms of surface modification, the surface properties of Ni can be changed by adding a trace noble metal. In addition, the surface reconstruction of the bimetallic particles can be caused by temperature or adsorbate [101,102]. GARCIÁ-DIÉGUEZG et al. [103] prepared a Ni-Pt bimetallic catalyst for a CRM reaction. Compared with the Ni catalyst, the Ni-Pt bimetallic catalyst formed a Ni-Pt alloy with higher activity and lower carbon deposition. Although only a small amount of precious metals was added to the Ni-based catalyst, the production cost of the catalyst still increased. Therefore, some researchers doped transition metals such as Co, Fe, and Cu into a Ni-based catalyst to construct a CRM bimetallic catalyst to reduce the industrial production cost [104]. Co, Fe, and Cu have a strong synergistic effect in the bimetallic system. Of course, the specific effects of the three metals are different [105–109]. Some researchers discussed the effect of Ni-Co, Ni-Fe, and Ni-Cu bimetallic catalysts. The introduction of the second active component, Co or Cu, into the Ni-based catalyst helped to improve the catalytic activity and carbon deposition resistance [110].

The Ni-Co bimetallic catalyst shows a stronger synergistic effect [111–113]. Additionally, the Ni/Co ratio, which can adjust the surface composition of Ni-Co clusters, plays a crucial role in the Ni-Co bimetallic system [114–117]. Generally, a small amount of Co can optimize the adjustment process, while excessive Co will cause the catalyst to be oxidized. The promotive effect of Co is mainly due to its strong affinity for oxygen species, enhancing the ability to eliminate carbon deposition on the catalyst [111,118,119]. The Ni-Co/Al_2O_3 bimetallic catalyst showed high thermal stability at 800 °C and effectively inhibited the side reaction of RWGS [120]. Turap et al. [84] prepared a Ni-Co/CeO_2 bimetallic catalyst for CRM reaction and found that the strong oxygen affinity of Co and the strong oxygen storage capacity of CeO_2 were helpful in eliminating carbon deposition. As the Co/Ni ratio was up to 0.8, the catalyst presented better activity and stability. Li et al. [121] studied the catalytic performance of a bimetallic Ni-Co/Al_2O_3 catalyst for CRM and found that the addition of metal Co can form a Ni-Co alloy, increasing the activation energy of CH_4 dissociation, thus inhibiting the CH_4 cracking activity. At the same time, the addition of Co could improve the oxygen affinity of the catalyst and remove carbon deposition. Liang et al. [122] used a one-pot method to synthesize an attapulgite-derived MFI (ADM) zeolite-coated Ni-Co alloy. The results showed that the Ni-Co alloy existed stably in the CRM process, which was conducive to the formation of electron-rich Ni metal and significantly improved the fracture ability of the C-H bond. At the same time, ADM not only firmly anchors metal sites through pore structure or layered system, but also provides rich CO_2 adsorption/activation centers, realizing high CRM reaction activity and improving the anti-carbon deposition performance.

Cu can partly replace Ni to improve catalyst activity and carbon deposition resistance [110]. Song et al. [123] constructed a Ni-Cu bimetallic catalyst. The catalyst with a 0.25–0.50 Cu/Ni ratio showed good activity, stability, and carbon deposition resistance, while the catalyst with higher and lower Cu/Ni ratios would be deactivated due to serious carbon deposition. The excellent performance of the optimized Ni-Cu/Mg(Al)O catalyst was related to the synergistic effect between Ni and Cu. On the one hand, the alloying of

Ni and Cu inhibited the deep dissociation of methane, and the carbon species obtained were more easily gasified (carbon eliminated). On the other hand, Cu provided active sites for the dissociation of CO_2, leading to the formation of active oxygen species. The alloying of Ni and Cu reduced the decomposition rate of CH_4, promoted the dissociation of CO_2, and effectively inhibited carbon deposition. Other studies showed that [124], during the CRM reaction, the addition of Cu had a significant effect on the activity and anti-carbon deposition performance of the Ni/CeO_2 catalyst, and the formation of a Ni-O-Ce solid solution generated more oxygen vacancies, improving catalytic activity.

Fe has always played a certain role in promoting the CRM reaction. Both Fe and Ni are iron elements with similar element properties, and the two metals can be alloyed in a certain proportion to make a catalyst with good catalytic performance [93,125]. The research from Kim et al. [126] showed that the catalysts supported solely with Ni or Fe presented the problems of fast deactivation and a low conversion rate, respectively, while the bimetallic Ni-Fe catalyst showed good activity and stability in the CRM reaction. By further analysis, it was found that the promotion of Fe in a Ni-Fe alloy was due to the cracking of CH_4 on the active metal Ni to produce H_2 and carbon. A part of Fe reacts with CO_2 to generate FeO, which falls off from the alloy. Additionally, the carbon can react with FeO and be oxidized to generate CO. Then, FeO is reduced to Fe, which is the original Ni-Fe alloy. This decarburization reaction cycle is conducive to the reducing of the surface carbon on the catalyst. The anti-carbon deposition performance of different bimetallic catalysts is shown in Table 2.

Table 2. Carbon deposition resistance of bimetallic catalysts in DRM.

Catalysts	SV /(mL·g^{-1}·h^{-1})	Feed Ratio	Temperature /K	CH_4 Conversion Rate /%	CO_2 Conversion Rate /%	Carbon Deposition /%
Ru-Ni/Al_2O_3 [127]	60,000		1023	94.00	97.00	0.32
Co-Ni/CeO_2 [84]	30,000	CH_4:CO_2 = 1:1	1073	80.10	82.20	10.00
NiFe/Al_2O_3 [128]	12,000	CH_4:CO_2 = 1:1	823	26.60	37.80	2.30
NiCu/Al_2O_3 [129]	18,000	CH_4:CO_2:He = 1:1:8	923	65.00	64.34	6.40
Ni-Co/Al_2O_3 [130]	54,000	CH_4:CO_2:N_2 = 2:2:1	1023	96.10	92.20	1.00
NiPt/Al_2O_3 [100]		CH_4:CO_2:Ar = 45:45:10	1023	86.00	87.00	7.00

Selection of Support

The support is a very important part of a catalyst. In a CO_2-CH_4 reforming reaction, the commonly used supports are Al_2O_3, MgO, CeO_2, TiO_2, SiO_2, etc. Although the support itself has no activity in the reaction, it can change the overall performance of the catalyst. The physical and chemical properties of the support, such as surface morphology, pore structure, interaction with active component, and the resulting differences due to the support, such as surface–interface structure, surface composition, grain size, and dispersion of the active component, can affect the existence form of the active component precursor and the catalyst activity, selectivity, stability, and carbon deposition resistance. Many studies have pointed out that strong interaction between the support and the active component is conducive to improving the dispersion and sintering resistance of the active metal, resulting in a high carbon resistance performance.

The stronger the interaction between the support and the metal, the less likely the catalyst will be reduced. If it can be reduced under certain conditions, then the smaller the metal particles, the better the dispersion. The excessive surface acidity of the support leads to catalyst deactivation through methane decomposition. Similarly, excessive surface basicity leads to catalyst deactivation through the Boudouard reaction as well as through the formation of metal oxides [39]. Hao et al. [131] reported that a close combination of Ni and carrier caused by a strong metal-support interaction promoted the transfer of transition species at the interface and the transfer of electrons, leading to the transformation of non-inert carbon species in the reaction process and avoiding the forming of inert carbon deposition. At the same time, strong metal-support interaction can effectively inhibit the

sintering and growth of Ni particles under the reaction conditions and can have a certain stabilizing effect on Ni particles, thereby improving the performance of the catalyst. Liu et al. [60] found through their research that Ni/CeO_2 was very active in the CRM reaction and that strong metal-support interaction enhanced the dissociation reaction activity of Ni to CH_4 and inhibited the formation of carbon deposition. Ruckenstein et al. [132] prepared a Ni/TiO_2 catalyst and found that there was a strong interaction between Ni and TiO_2, which led to the reduction in the free energy of the system. TiO_x can promote the elimination of carbon to a certain extent, but TiO_x molecules migrate on the surface during the reduction process, covering the active sites of Ni. A large amount of filamentous carbon was formed on Ni supported on CeO_2 and on CeO_2 doped with iso-valent Zr, while a negligible amount was formed on Ni supported on CeO_2 doped with aliovalent Sm or La (Figure 7). The ceria dopants can change the interaction of Ni with the support [133].

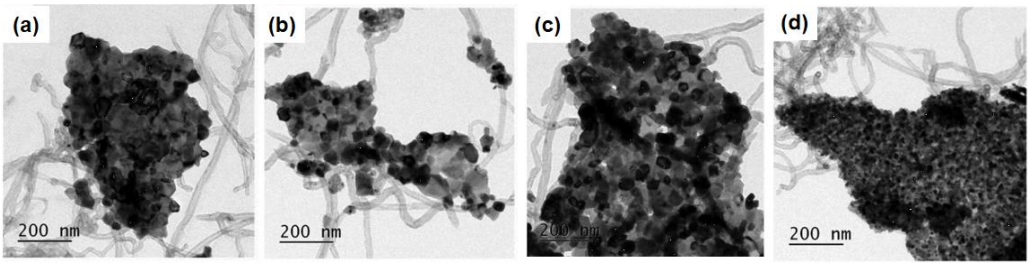

Figure 7. Bright field TEM images (**a**–**d**) [133].

The pore structure of the support has a great influence on the performance of the catalyst and has a limited domain effect on the active component. It has been found that micropores (<2nm) are not conducive to the dispersion of metal particles; mesopores (2–50 nm) can make the catalyst have a large specific surface area; macropores (>50nm) can promote the diffusion of reactant and product molecule, make gas molecules fully contact the catalyst, and increase the number of exposed Ni active sites [134]. Due to the limitation of the mesoporous structure of the support, Ni particles exist in the pores on the catalyst as much as possible, with high dispersion, which is conducive to strong metal-support interaction, thus reducing the formation of carbon deposition [135]. The catalyst with multistage pore structure has higher carbon capacity and a lower carbon deposition deactivation rate due to the addition of different levels of pores [134,136]. Du et al. [137] reported a CRM catalyst of HT-NiMgAl with a multistage pore structure. The multistage pore structure of this catalyst effectively increased the specific surface area of the catalyst, improving the dispersion of Ni particles; it could effectively inhibit carbon deposition due to its role in limiting the region of the active component.

After the reduction in the catalyst, the Ni atoms are easily sintered at high temperature, which leads to the reduction in the dispersion of Ni atoms on the surface and the increase in the concentration difference between the bulk Ni atoms and the surface Ni atoms so that the Ni atoms dissolved in the support will migrate to the surface under the promotion of the concentration gradient, supplementing the dispersion of the surface Ni atoms. Studies showed that the Co/MgO catalyst provides a strong Lewis alkaline environment due to the formation of solid solution $CoMgO_x$, which effectively stabilizes the Co nanoparticles on the surface of the support. Due to the alternating polar nanolayer structure of O^{2-} and Mg^{2+} and the existence of a large number of O^{2-} Lewis alkaline sites on the surface of MgO(111), the anti-sintering ability and anti-carbon deposition performance of the catalyst have been improved [138,139]. In addition, the support has a Lewis base, which can increase the alkalinity of the catalyst, promote the adsorption and dissociation of CO_2, and eliminate carbon deposition in the reaction. At the same time, the alkalinity of the support can inhibit the growth of Ni metal particles at high temperatures, thus improving the activity, stability, and carbon deposition resistance of the catalyst [140]. Jafarbegloo et al. [141] prepared a NiO-MgO catalyst and found that the strong Lewis base of MgO absorbed a large amount

of carbon dioxide, improved the conversion rate of carbon dioxide, and eliminated carbon deposition on the catalyst surface.

Li et al. [142] prepared an iron-rich biomass-derived carbon for the CO_2-CH_4 reforming and found that it had higher activity than non-iron-rich carbon. Before 800 °C, the order of the iron-rich carbon promoting the reforming reaction was followed by Fe-C_2 (10% Fe content) > Fe-C_3 (20% Fe content) > Fe-C_1 (5% Fe content). After 800 °C, Fe-C_2 can still achieve the maximum CH_4 conversion rate. In addition, the catalytic activity of Fe-C_2 to CH_4 at 800 °C was better than that of other catalysts at higher temperature. By further measuring the carbon catalyst used, it was found that the weights of iron-rich carbon and non-iron-rich carbon increased by 0.2% and 0.9%, respectively. Therefore, it can be proved that the carbon deposition on the carbon catalyst is less, which effectively eliminates the carbon deposition. After the test, the iron-rich carbon had less carbon deposition, mainly in the form of filamentous carbon, which was more easily removed by carbon removal reaction.

Most biomass carbons are alkaline, and their ash contains a large amount of alkali metals (K, Na) and alkaline earth metals (Ca, Mg), which can promote the formation of alkaline sites, facilitate the adsorption and dissociation of CO_2, and inhibit the formation of carbon deposition. It has been reported that alkali/alkaline earth metals are one of the main reasons for biomass carbon to promote CO_2-CH_4 reforming [142]. Zhang et al. [143] studied the role of alkali/alkaline earth metals in tar reforming. The results showed that alkali/alkaline earth metals promoted the interaction between the active metal Ni and the carrier and inhibited the sintering of Ni. Alkali/alkaline earth metals cause more oxygen to be adsorbed on the surface of the catalyst, which has strong oxidizability. It can react with reaction intermediates or C, avoid the deposition of C on the catalyst, and inhibit carbon deposition [142–144]. San et al. [145] studied the role of alkali metal K and speculated that K can promote C gasification reaction and cover some active sites to inhibit CH_4 decomposition and reduce carbon deposition, but the coverage of active sites will also have a certain negative impact on the reforming reaction. Wu et al. [146] used CaO as the carrier to theoretically calculate that the presence of CaO adsorbed more CO_2 to the participate in the CO_2-CH_4 reforming and that CO_2 dissociated at the interface between Ni and CaO; in addition, the oxygen species produced by dissociation and carbon deposition on the surface of the catalyst generated CO, which extended the service life of the catalyst.

Application of Confined Catalyst

A confined catalyst can effectively confine the active center on the catalyst in different ways, which mainly include lattice limit, pore limit, core-shell limit, surface space limit, and multiple limits.

Lattice confinement can effectively anchor precious metal or non-precious metal on the regularly arranged spatial skeleton and can improve the dispersion of active centers. Ruitenbeek et al. [147] used a catalyst composed of a single iron atom in the lattice confined region; it had high activity and selectivity in the reaction and almost no carbon deposition. The surface confined catalyst had a high specific surface area, highly ordered pore structure, and narrow pore size distribution. Wang et al. [148] used dendritic mesoporous SiO_2 (DMS) as a carrier to prepare an alkali metal oxide modified low-temperature carbon deposition-resistant Ni-based catalyst and applied it to a reforming reaction, which showed excellent low-temperature carbon deposition resistance.

Kong et al. [149] prepared microporous molecular sieve S-1 with rich pores and high specific surface area, and effectively embedded the active component Ni in the pores and applied it to CO_2-CH_4 reforming. The results showed that the catalyst had excellent activity and stability at 650 °C and 0.5 MPa for 100 h. The thermogravimetric test of the catalyst after reaction did not find weight loss and indicated that the S-1-encapsulated Ni-based catalyst had excellent carbon deposition resistance. The main reason was that the catalyst channel effectively restricted the aggregation of Ni particles, which made the Ni disperse uniformly and reduced the size of the Ni.

Core-shell catalysts mainly include two types: one is the close contact type; the other is the eggshell type (the active component is separated from the shell). Zhang et al. [150] wrapped the perovskite $LaNiO_3$ nano-cube in the mesoporous silica shell to form a new core-shell structure catalyst, which was used in the CO_2-CH_4 reforming and showed excellent carbon deposition resistance. Compared with the eggshell catalyst, the core-shell catalyst had a contact interface between the core and shell, which resulted in enhanced interaction, inhibition of the movement of the active center, and reduction in the particle size. Liu et al. [151] designed a high-performance In-Ni@SiO_2 close-contact nanocore-shell catalyst. The In-Ni@SiO_2 catalyst had higher activity compared to the Ni@SiO_2 catalyst. CO_2 and CH_4 reacted at 800 °C for 430 h and still maintained 90% conversion. After reaction, compared with the other supported catalyst, they had less carbon deposition, better stability, and anti-carbon deposition performance.

Multiple restriction can limit the active center, reduce its exposure, and improve carbon deposition resistance on the catalyst. Wang et al. [152] prepared a Ni@La_2O_3/SiO_2 catalyst, and the results showed that an amorphous La_2O_3 layer was coated on the SiO_2, while small Ni nanoparticles were encapsulated in the La_2O_3 layer. As Ni nanoparticles were encapsulated in the La_2O_3 amorphous layer, it could effectively inhibit the formation of carbon deposition in CO_2-CH_4 reforming.

4.2.2. Eliminate Carbon Deposition from Process Condition Matching

The conversion rate of carbon dioxide and methane varies with the ratio of reaction gas, space velocity, reactor size, and catalyst dosage.

Selection of Operating Conditions (Temperature, Pressure, etc.)

Nematollahi et al. [153] conducted the same thermodynamic simulation under different pressures and found that the conversion rate of CH_4 and CO_2 and the amount ratio of the H_2/CO substances decreased significantly with the increase in operating pressure. This is due to the fact that the CRM reforming is a reaction with an increase in volume. The lower the pressure, the better the reaction. The high-pressure environment inhibits the conversion of the reactants. Some researchers conducted thermodynamic simulation on the influence of temperature, CH_4/CO_2 ratio, reaction pressure, and other oxidants on the formation of carbon deposition and proposed that high conversion and less carbon deposition could be obtained by operating at a high temperature, low pressure, and high CH_4/CO_2 ratio above 850 °C [17,154,155]. Bao et al. [156] prepared a NiCeMgAl double-porous (mesoporous–mesoporous) catalyst. When the space velocity was lower than 96,000 h^{-1}, the larger mesopores provides a fast transport channel for the reactants and product molecules. At a higher space velocity (such as 120,000 h^{-1}), the conversion rate was reduced because the reactants could not fully diffuse to the active center in the catalyst. The thermogravimetric analysis results showed that with the (Ni_{15}CeMgAl) the total weight loss of the dual porous catalyst after reaction was 16.8%, of which amorphous carbon accounted for 2.5%, carbon nanotubes accounted for 9%, graphite-like carbon accounted for 1%, and the others comprised the desorption of adsorbed small molecules. It was further found that carbon nanotubes could act as a carrier to continue the reaction and prolong the service life of the catalyst.

Adjustment and Matching of Reaction Gases

Carbon species deposited on the catalyst surface can usually be eliminated by the oxidation of CO_2 through the carbon elimination reaction ($CO_2 + C \rightarrow 2CO$). Therefore, the total amount of carbon deposition on the catalyst depends on the balance between methane cracking, carbon monoxide disproportionation, and the decarburization reaction [63], which can be considered from the two aspects of the inhibition of the carbon deposition reaction and the promotion of the decarburization reaction to improve the anti-carbon deposition performance of the catalyst. Of course, increasing the proportion of CO_2 can inhibit the formation of carbon deposition but increasing the proportion of CO_2 will promote the

occurrence of side reactions and lead to increased separation costs in the later period. Therefore, the determination of the CO_2/CH_4 ratio should be combined with various factors. Mo et al. [49] found that with the increase in the CO_2/CH_4 ratio, the amount of carbon deposition on the catalyst surface gradually decreased, and the area and intensity of the high-temperature hydrogenation peak gradually weakened, indicating that low activity β carbon was significantly reduced due to the increase in the proportion of CO_2. The results also showed that the addition of CO_2 played an important role in preventing the transformation from active carbon to inactive carbon.

Adding steam or oxygen to the reaction for mixed reforming can also reduce carbon deposition on the catalyst. Li et al. [157] prepared a Ni/CeO_2-ZrO_2-Al_2O_3 catalyst, carried out a CO_2-CH_4 reforming reaction with and without steam, and measured the amount of carbon deposition. The results showed that the addition of steam to the reaction gas could significantly reduce the carbon deposition, improving the stability of the catalytic reaction. O'Connor et al. [158] found that the Ni/Al_2O_3 catalyst had high activity at 550–800 °C under the conditions of CO_2 reforming and the partial oxidation of methane. With the increase in the O_2 addition, almost no surface carbon deposition was found, but the activity of the catalyst decreased with time.

LI et al. [159] conducted a study employing the action of microwave-irradiated biological semi-coke; the experimental study of CO_2/steam-combined CH_4 reforming was carried out. The characteristics of the combined reforming reaction were examined, and the effects of the combined reforming reaction on the quality of the syngas, the loss of biochar, the surface characteristics, and the functional groups were discussed. The results showed that the combined reforming reaction could promote the conversion of the reaction gas, causing the the average value of the volume ratio of H_2/CO in the syngas to be within 90, the min reaction time to rise to 0.923, and the H_2/CO gas volume ratio to be closer to 1.

5. Conclusions and Prospect

CRM reforming not only promotes the utilization of CH_4 and CO_2 but also plays an important role in mitigating the greenhouse effect and reducing carbon emissions. It is an effective means of achieving carbon peaking and carbon neutralization and has good industrial value and application prospects. The key to the stable operation of the reaction is the construction of the catalyst, and the easy sintering of the active component and carbon deposition on the catalyst in the reaction is the core problem that needs to be solved urgently. As the preferred catalyst for this reaction, the Ni-based catalyst also faces the above problems. This paper briefly introduces the thermodynamics, kinetics, and reaction mechanism of the CRM reaction and focuses on the research progress of carbon deposition and carbon elimination on the used catalysts. The following prospects are put forward in terms of inhibiting carbon deposition in order to improve the activity and stability of the CRM catalyst:

1. More advanced characterization methods should be used to explore the reaction mechanism and carbon deposition mechanism of the CRM reaction on a Ni-based catalyst, and the reaction mechanism and anti-carbon deposition mechanism of the Ni-based catalyst should be further clarified.
2. By introducing different types of additives to regulate the number of alkaline sites on the surface of the catalyst, the adsorption performance of CO_2 may be enhanced, and more adsorbed oxygen may be generated; the gasification process of the carbon deposition may also be promoted.
3. By DFT or other calculations, the formation and elimination mechanism of carbon deposition can be discussed in depth, and the catalyst design scheme can correspondingly be optimized to inhibit carbon deposition.

Funding: This work was supported by the natural science foundation of Xinjiang Uyghur Autonomous Region (2022D01C23), the Ningxia natural science foundation (2022AAC03307), the high quality development special project for science and technology supporting industry from Changji (2022Z04), and the special project for the central government to guide local scientific and technological development (ZYYD2022C16).

Data Availability Statement: No new data were created or analyzed in this study. Data sharing is not applicable to this article.

Conflicts of Interest: The authors declare no conflict of interest.

References

1. Liu, Q.; Wang, S.J.; Zhao, G.M.; Yang, H.Y.; Yuan, M.; An, X.X.; Zhou, H.F.; Qiao, Y.Y.; Tian, Y.Y. CO_2 methanation over ordered mesoporous NiRu-doped CaO-Al_2O_3 nanocomposites with enhanced catalytic performance. *Int. J. Hydrogen Energy* **2018**, *43*, 239–250. [CrossRef]
2. Zain, M.M.; Mohamed, A.R. An overview on conversion technologies to produce value added products from CH_4 and CO_2 as major biogas constituents. *Renew. Sustain. Energy Rev.* **2018**, *98*, 56–63. [CrossRef]
3. Lougou, B.G.; Shuai, Y.; Chaffa, G.; Xing, H.; Tan, H.P.; Du, H.B. Analysis of CO_2 utilization into synthesis gas based on solar thermochemical CH_4-reforming. *J. Energy Chem.* **2019**, *28*, 61–72. [CrossRef]
4. Bradford, M.C.J.; Vannice, M.A. Catalytic reforming of methane with carbon dioxide over nickel catalysts II. Reaction kinetics. *Appl. Catal. A Gen.* **1996**, *142*, 97–122. [CrossRef]
5. Oezkara-Aydmoglu, S. Thermodynamic equilibrium analysis of combined carbon dioxide reforming with steam reforming of methane to synthesis gas. *Int. J. Hydrogen Energy* **2010**, *35*, 12821–12828. [CrossRef]
6. Kang, J.; He, S.; Zhou, W.; Shen, Z.; Li, Y.Y.; Chen, M.S.; Zhang, Q.H.; Wang, Y. Single-pass transformation of syngas into ethanol with high selectivity by triple tandem catalysis. *Nat. Commun.* **2020**, *11*, 827. [CrossRef]
7. Kawi, S.; Kathiraser, Y.; Ni, J.; Oemar, U.; Li, Z.W.; Saw, E.T. Progress in Synthesis of Highly Active and Stable Nickel-Based Catalysts for Carbon Dioxide Reforming of Methane. *ChemSusChem* **2015**, *8*, 3556–3575. [CrossRef]
8. Oyama, S.; Hacarlioglu, P.; Gu, Y.; Lee, D. Dry reforming of methane has no future for hydrogen production: Comparison with steam reforming at high pressure in standard and membrane reactors. *Int. J. Hydrogen Energy* **2012**, *37*, 10444–10450. [CrossRef]
9. Qin, Z.; Chen, J.; Xie, X.; Luo, X.; Su, T.M.; Ji, H.B. CO_2 reforming of CH_4 to syngas over nickel-based catalysts. *Environ. Chem. Lett.* **2020**, *18*, 997–1017. [CrossRef]
10. Abdulrasheed, A.; Jalil, A.A.; Gambo, Y.; Ibrahim, M.; Hambali, H.U.; Hamid, M.Y.S. A review on catalyst development for dry reforming of methane to syngas: Recent advances. *Renew. Sustain. Energy Rev.* **2019**, *108*, 175–193. [CrossRef]
11. Pakhare, D.; Spivey, J. A review of dry (CO_2) reforming of methane over noble metal catalysts. *Chem. Soc. Rev.* **2014**, *43*, 7813–7837. [CrossRef]
12. Li, W.Y.; Feng, J.; Xie, K.C.; Sun, Q. Study on carbon deposition performance of nickel catalyst for CH_4-CO_2 reforming reaction. *J. Fuel Chem. Technol.* **1997**, *25*, 460–464.
13. Li, X.C.; Li, S.G.; Yang, Y.F.; Wu, M.; He, F. Study on Coke Formation and Stability of Nickel-Based Catalysts in CO_2 Reforming of CH_4. *Catal. Lett.* **2007**, *118*, 59–63.
14. Ji, L.; Tang, S.; Zeng, H.C.; Lin, J.; Tan, K.L. CO_2 reforming of methane to synthesis gas over sol-gel-made Co/γ-Al_2O_3 catalysts from organometallic precursors. *Appl. Catal. A Gen.* **2001**, *207*, 247–255. [CrossRef]
15. Xu, Z.; Li, Y.; Zhang, J.Y.; Chang, L.; Zhou, R.Q.; Duan, Z.T. Bound-state Ni species-a superior form in Ni-based catalyst for CO_2-CH_4 reforming. *Appl. Catal. A Gen.* **2001**, *210*, 45–53. [CrossRef]
16. Yang, Y.L.; Xu, H.Y.; Li, W.Z. Pyrolysis and deposition performance of CH_4, C_2H_6 and C_2H_4 on Ni-based catalysts. *Acta Phys. Chim. Sin.* **2001**, *17*, 773–775. [CrossRef]
17. Zhang, J.; Wang, H.; Dalai, A.K. Development of stable bimetallic catalysts for carbon dioxide reforming of methane. *J. Catal.* **2007**, *249*, 300–310. [CrossRef]
18. Fraenkel, D.; Levitan, R.; Levy, M. A solar thermochemical pipe based on the CO_2-CH_4 (1:1) system. *Int. J. Hydrogen Energy* **1986**, *11*, 267–277. [CrossRef]
19. Wang, S.B.; Lu, G.Q.; Millar, G.J. Carbon Dioxide Reforming of Methane to Produce Synthesis Gas over Metal-Supported Catalysts: State of the Art. *Energy Fuels* **1996**, *10*, 896–904. [CrossRef]
20. Abdullah, B.; Ghani, N.A.A.; Vo, D.-V.N. Recent advances in dry reforming of methane over Ni-based catalysts. *J. Clean. Prod.* **2017**, *162*, 170–185. [CrossRef]
21. Al-Fatesh, A.; Singh, S.K.; Kanade, G.S.; Atia, H.; Fakeeha, A.H.; Ibrahim, A.A.; El-Toni, A.M.; Labhasetwar, N.K. Rh promoted and ZrO_2/Al_2O_3 supported Ni/Co based catalysts: High activity for CO_2 reforming, steam-CO_2 reforming and oxy-CO_2 reforming of CH_4. *Int. J. Hydrogen Energy* **2018**, *43*, 12069–12080. [CrossRef]
22. Oemar, U.; Kathiraser, Y.; Mo, L.; Ho, X.K.; Kawi, S. CO_2 reforming of methane over highly active La-promoted Ni supported on SBA-15 catalysts: Mechanism and kinetic modelling. *Catal. Sci. Technol.* **2016**, *6*, 1173–1186. [CrossRef]

23. Assabumrungrat, S.; Charoenseri, S.; Laosiripojana, N.; Kiatkittipong, W.; Praserthdam, P. Effect of oxygen addition on catalytic performance of Ni/SiO_2·MgO toward carbon dioxide reforming of methane under periodic operation. *Int. J. Hydrogen Energy* **2009**, *34*, 6211–6220. [CrossRef]
24. Wang, Z.J.; Song, H.; Liu, H.; Ye, J. Coupling of Solar Energy and Thermal Energy for Carbon Dioxide Reduction: Status and Prospects. *Angew. Chem. Int. Ed.* **2020**, *59*, 8016–8035. [CrossRef]
25. Paksoy, A.I.; Caglayan, B.S.; Aksoylu, A.E. An in situ FTIR-DRIFTS study on CDRM over Co-Ce/ZrO_2: Active surfaces and mechanistic features. *Int. J. Hydrogen Energy* **2020**, *45*, 12822–12834. [CrossRef]
26. Bodrov, N.N.; Apelbaum, L.O.; Temkin, M.I. Kinetics of the reaction of methane with steam on the surface of nickel. *Kinet. Catal.* **1964**, *5*, 614–621. [CrossRef]
27. Rostrupnielsen, J.R.; Hansen, J.H.B. CO_2-Reforming of Methane over Transition Metals. *J. Catal.* **1993**, *144*, 38–49. [CrossRef]
28. Osaki, T.; Masuda, H.; Mori, T. Intermediate hydrocarbon species for the CO_2-CH_4 reaction on supported Ni catalysts. *Catal. Lett.* **1994**, *29*, 33–37. [CrossRef]
29. Bradford, M.C.J.; Vannice, M.A. CO_2 reforming of CH_4 over supported Pt catalysts. *J. Catal.* **1998**, *173*, 157–171. [CrossRef]
30. Wei, J.M.; Iglesia, E. Isotopic and kinetic assessment of the mechanism of reactions of CH_4 with CO_2 or H_2O to form synthesis gas and carbon on nickel catalysts. *J. Catal.* **2004**, *224*, 370–383. [CrossRef]
31. Wang, S.G.; Liao, X.Y.; Jia, H.; Cao, D.B.; Li, Y.W.; Wang, J.; Jiao, H. Kinetic aspect of CO_2 reforming of CH_4 on Ni(111): A density functional theory calculation. *Surf. Sci.* **2007**, *601*, 1271–1284. [CrossRef]
32. Wang, S.G.; Liao, X.Y.; Cao, D.B.; Li, Y.W.; Wang, J.G.; Jiao, H.J. Formation of Carbon Species on Ni(111): Structure and Stability. *J. Phys. Chem. C* **2007**, *111*, 10894–10903. [CrossRef]
33. Freund, H.J.; Messmer, R.P. On the bonding and reactivity of CO_2 on metal surfaces. *Surf. Sci. Lett.* **1986**, *172*, 1–30. [CrossRef]
34. Muhammad, A.; Tahir, M.; Al-Shahrani, S.S.; Ali, A.M.; Rather, S.U. Template free synthesis of graphitic carbon nitride nanotubes mediated by lanthanum (La/g-CNT) for selective photocatalytic CO_2 reduction via dry reforming of methane (DRM) to fuels. *Appl. Surf. Sci.* **2020**, *504*, 144177. [CrossRef]
35. Xie, W.; Liang, D.; Li, L.; Qu, S.J.; Tao, W. Surface chemical ploperties and pore structure of the activated coke and their effects on the denitrification activity of selective catalytic reduction. *Int. J. Coal Sci. Technol.* **2019**, *6*, 595–602. [CrossRef]
36. Khavarian, M.; Chai, S.P.; Mohamed, A.R. Direct use of as-synthesized multi-walled carbon nanotubes for carbon dioxide reforming of methane for prodacing synthesis gas. *Chem. Eng. J.* **2014**, *257*, 200–208. [CrossRef]
37. He, L.; Hu, S.; Yin, X.; Jun, X.; Han, H.D.; Li, H.J.; Ren, Q.Q.; Su, S.; Wang, Y.; Xiang, J. Promoting effects of Fe-Ni alloy on co-production of H_2 and carbon nanotubes during steam reforming of biomass tar over Ni-Fe/α-Al_2O_3. *Fuel* **2020**, *276*, 118116. [CrossRef]
38. Ma, Q.X.; Wang, D.; Wu, M.B.; Zhao, T.S.; Yoneyama, Y.; Tsubaki, N. Effect of catalyticsite position: Nickel nanocatalyst selectively loaded inside or outside carbon nanotubes for methane dry reforming. *Fuel* **2013**, *108*, 430–438. [CrossRef]
39. Das, S.; Sengupta, M.; Patel, J.; Bordoloi, A. A study of the synergy between support surface properties and catalyst deactivation for CO_2 reforming over supported Ni nanoparticles. *Appl. Catal. A Gen.* **2017**, *545*, 113–126. [CrossRef]
40. Zhang, M.; Zhang, J.F.; Wu, Y.Q.; Pan, J.X.; Zhang, Q.D.; Tan, Y.S.; Han, Y.Z. Insight into the effects of the oxygen species over Ni/ZrO_2 catalyst surface on methane reforming with carbon dioxide. *Appl. Catal. B Environ.* **2019**, *244*, 427–437. [CrossRef]
41. Jin, B.T.; Li, S.G.; Liang, X.H. Enhanced activity and stability of MgO-promoted Ni/Al_2O_3 catalyst for dry reforming of methane: Role of MgO. *Fuel* **2021**, *284*, 119082. [CrossRef]
42. Wang, Y.N.; Zhang, R.J.; Yan, B.H. Ni/$Ce_{0.9}Eu_{0.1}O_{1.95}$ with enhanced coke resistance for dry reforming of methane. *J. Catal.* **2022**, *407*, 77–89. [CrossRef]
43. Burghaus, U. Surface science perspective of carbon dioxide chemistry-Adsorption kinetics and dynamics of CO_2 on selected model surfaces. *Catal. Today* **2009**, *148*, 212–220. [CrossRef]
44. Pan, Y.X.; Liu, C.J.; Wiltowski, T.S.; Ge, Q.F. CO_2 adsorption and activation over γ-Al_2O_3-supported transition metal dimers: A density functional study. *Catal. Today* **2009**, *147*, 68–76. [CrossRef]
45. Tsipouriari, V.A.; Verykios, X.E. Carbon and Oxygen Reaction Pathways of CO_2 Reforming of Methane over Ni/La_2O_3 and Ni/Al_2O_3 Catalysts Studied by Isotopic Tracing Techniques. *J. Catal.* **1999**, *187*, 85–94. [CrossRef]
46. Daza, C.E.; Gallego, J.; Mondragon, F.; Moreno, S.; Molina, R. High stability of Ce-promoted Ni/Mg-Al catalysts derived from hydrotalcites in dry reforming of methane. *Fuel Guildf.* **2010**, *89*, 592–603. [CrossRef]
47. Liu, C.J.; Ye, J.Y.; Jiang, J.J.; Pan, Y.X. Progresses in the preparation of coke resistant Ni-based catalyst for steam and CO_2 reforming of methane. *ChemSusChem* **2011**, *3*, 529–541.
48. Ferreira-Aparicio, P.; Fernandez-Garcia, M.; Guerrero-Ruiz, A.; Rodriguez-Ramos, I. Evaluation of the role of the metal-support interfacial centers in the dry reforming of methane on alumina-supported rhodium catalysts. *J. Catal.* **2000**, *190*, 296–308. [CrossRef]
49. Mo, W.L.; Ma, F.Y.; Liu, J.M.; Zhong, M.; Nulahong, A.S. Study on CO_2-CH_4 reforming reaction carbon deposition on Ni-Al_2O_3 catalyst based on programmed hydrogenation characterization. *J. Fuel Chem. Technol.* **2019**, *47*, 549–557.
50. Mo, W.L.; Ma, F.Y.; Liu, Y.E.; Liu, J.M.; Aisha, N. Preparation of porous Al_2O_3 by template method and its application in Ni-based catalyst for CH_4/CO_2 reforming to produce syngas. *Int. J. Hydrogen Energy* **2015**, *40*, 16147–16158. [CrossRef]
51. Wang, C.Z.; Sun, N.N.; Wei, W.; Zhang, Y.X. Carbon intermediates during CO_2 reforming of methane over Ni-CaO-ZrO_2 catalysts: Atemperature-programmed surface reaction study. *Int. J. Hydrogen Energy* **2016**, *41*, 19014–19024. [CrossRef]

52. Bodrov, I.M.; Apelbaum, L.O. Reaction kinetics of methane and carbon dioxide on a nickel surface. *Kinet. Catal.* **1967**, *8*, 379.
53. Li, D.L.; Xu, S.P.; Song, K.; Chen, C.Q.; Zhan, Y.Y.; Jiang, L.L. Hydrotalcite-derived Co/Mg(Al)O as a stable and coke-resistant catalystfor low-temperature carbon dioxide reforming of methane. *Appl. Catal. A Gen.* **2018**, *552*, 21–29. [CrossRef]
54. Wang, R.; Xu, H.Y.; Liu, X.B.; Ge, Q.J.; Li, W.Z. Role of redox couples of $Rh^0/Rh^{\delta+}$and Ce^{4+}/Ce^{3+}in CO_2-CH_4 reforming over Rh-CeO_2/Al_2O_3 catalyst. *Appl. Catal. A Gen.* **2006**, *305*, 204–210. [CrossRef]
55. Ruckenstein, E.; Wang, H.Y. Carbon deposition and catalytic deactivation during CO_2 reforming of CH_4 over Co/γ-Al_2O_3 catalysts. *J. Catal.* **2002**, *205*, 289–293. [CrossRef]
56. Liang, T.Y.; Lin, C.Y.; Chou, F.C.; Wang, M.Q.; Tsai, D.H. Gas-phase synthesis of Ni-CeO_x hybrid nanopaticles and their synergistic catalysis for simultaneous reforming of methane and carbon dioxide to syngas. *J. Phys. Chem. C* **2018**, *122*, 11789–11798. [CrossRef]
57. Kuijpers, E.G.M.; Breedijk, A.K.; Van Der Wal, W.J.J.; Geus, J.W. Chemisorption of Methane on Ni/SiO_2 Catalysts and Reactivity of the Chemisorption Products toward Hydrogen. *J. Catal.* **1983**, *81*, 429–439. [CrossRef]
58. Osaki, T.; Masuda, H.; Horiuchi, T.; Mori, T. Highly hydrogen-deficient hydrocarbon species for the CO_2-reforming of CH_4 on Co/Al_2O_3 catalyst. *Catal. Lett.* **1995**, *34*, 59–63. [CrossRef]
59. Wang, Y.; Yao, L.; Wang, Y.N.; Wang, S.H.; Zhao, Q.; Mao, D.H.; Hu, C.W. Low-Temperature Catalytic CO_2 Dry Reforming of Methane on Ni-Si/ZrO_2 Catalyst. *ACS Catal.* **2018**, *8*, 6495–6506. [CrossRef]
60. Liu, Z.Y.; Lustemberg, P.; Gutierrez, R.A.; Carey, J.J.; Palomino, R.M.; Vorokhta, M.; Grinter, D.C.; Ramirez, P.J.; Matolin, V.; Nolan, M.; et al. In situ Investigation of Methane Dry Reforming on M-CeO_2(111) {M=Co, Ni, Cu} Surfaces: Metal-Support Interactions and the activation of C-H bonds at Low Temperature. *Angew. Chem. Int. Ed.* **2017**, *56*, 13041–13046. [CrossRef]
61. Liu, Z.Y.; Grinter, D.C.; Lustemberg, P.G.; Nguyen-Phan, T.-D.; Zhou, Y.H.; Luo, S.; Waluyo, I.; Crumlin, E.J.; Stacchiola, D.J.; Zhou, J.; et al. Dry Reforming of Methane on a Highly-Active Ni-CeO Catalyst: Effects of Metal-Support Interactions on C-H Bond Breaking. *Angew. Chem. Int. Ed.* **2016**, *55*, 7455–7459. [CrossRef]
62. Horiuchi, T.; Sakuma, K.; Fukui, T.; Kubo, Y.; Osaki, T.; Mori, T. Suppression of carbon deposition in the CO_2-reforming of CH_4 by adding basic metal oxides to a Ni/Al_2O_3 catalyst. *Appl. Catal. A* **1996**, *144*, 111–120. [CrossRef]
63. Gallego, G.S.; Batiot-Dupeyrat, C.; Barraault, J.; Florez, E.; Mondragon, F. Dry reforming of methane over $LaNi_{1-y}B_yO_{3\pm\delta}$ (B=Mg, Co) perovskites used as catalyst precursor. *Appl. Catal. A Gen.* **2008**, *334*, 251–258. [CrossRef]
64. Garcia-Dieguez, M.; Pieta, I.S.; Herrera, M.C.; Larrubia, M.A.; Malpartida, I.; Alemany, L.J. Transient study of the dry reforming of methane over Pt supported on different γ-Al_2O_3. *Catal. Today* **2010**, *149*, 380–387. [CrossRef]
65. Lucreda, F.; Assafj, M.; Assafe, M. Methane Conversion Reactions on Ni Catalysts Promoted with Rh: Influence of Support. *Appl. Catal. A Gen.* **2011**, *400*, 156–165. [CrossRef]
66. Xu, J.K.; Zhou, W.; Wang, J.H.; Li, Z.J.; Ma, J.X. Characterization and analysis of carbon deposited during the dry reforming of methane over Ni/La_2O_3/Al_2O_3 catalysts. *Chin. J. Catal.* **2009**, *30*, 1076–1084. [CrossRef]
67. Crnivec IG, O.; Djinovic, P.; Erjavec, B.; Pintar, A. Effect of synthesis parameters on morphology and activity of bimetallic catalysts in CO_2-CH_4 reforming. *Chem. Eng. J.* **2012**, *207*, 299–307. [CrossRef]
68. Liu, Z.C.; Zhou, J.; Cao, K.; Yang, W.M.; Gao, H.X. Highly dispersed nickel loaded on mesoporous silica: One-spot synthesis strategy and high performance as catalysts for methane reforming with carbon dioxide. *Appl. Catal. B Environ.* **2012**, *125*, 324–330. [CrossRef]
69. Guo, Y.P.; Feng, J.; Li, W.Y. Effect of the Ni size on CO_2-CH_4 reforming over Ni/MgO catalyst: A DFT study. *Chin. J. Chem. Eng.* **2017**, *25*, 1442–1448. [CrossRef]
70. Mo, W.L.; Ma, F.Y.; Ma, Y.Y.; Fan, X. The optimization of Ni-Al_2O_3 catalyst with the addition of La_2O_3 for CO_2-CH_4 reforming to produce syngas. *Int. J. Hydrogen Energy* **2019**, *44*, 24510–24524. [CrossRef]
71. Mo, W.L.; Ma, F.Y.; Liu, Y.E.; Liu, J.M.; Zhong, M.; Nulahong, A.S. Effect of preparation method on the catalytic performance of Ni-Al_2O_3 catalyst in CO_2-CH_4 reforming reaction. *J. Fuel Chem. Technol.* **2015**, *43*, 1083–1091.
72. Mo, W.L.; Ma, F.Y.; Liu, Y.E.; Liu, J.M.; Zhong, M.; Nulahong, A.S. Effect of roasting temperature on the performance of NiO/γ-Al_2O_3 catalyst for CO_2-CH_4 reforming syngas. *J. Inorg. Mater.* **2016**, *31*, 234–240.
73. Ding, R.G.; Yan, A.F. Structure characterization of the Co and Ni catalysts for carbon dioxide reforming of methane. *Catal. Today* **2001**, *68*, 135–143. [CrossRef]
74. Osaki, T.; Mori, T. Role of Potassium in Carbon-Free CO_2 Reforming of Methane on K-Promoted Ni/Al_2O_3 Catalysts. *J. Catal.* **2001**, *204*, 89–97. [CrossRef]
75. Wang, H.H.; Mo, W.L.; He, X.Q.; Fan, X.; Ma, F.Y.; Liu, S.; Tax, D. Effect of Ca Promoter on the Structure, Performance, and Carbon Deposition of Ni-Al_2O_3 Catalyst for CO_2-CH_4 Reforming. *ACS Omega* **2020**, *5*, 28955–28964. [CrossRef]
76. Wang, J.B.; Kuo, L.E.; Huang, T.J. Study of carbon dioxide reforming of methane over bimetallic Ni-Cr/yttria-doped ceria catalysts. *Appl. Catal. A Gen.* **2003**, *249*, 93–105. [CrossRef]
77. Potdar, H.S.; Roh, H.S.; Jun, K.W. Carbon Dioxide Reforming of Methane Over Co-precipitated Ni-CeO_2, Ni-ZrO_2, Ni-Ce-ZrO_2 Catalysts. *Catal. Today* **2004**, *93–95*, 39–44.
78. Roh, H.S.; Jun, K.W.; Baek, S.C.; Park, S.E. A Highly Active and Stable Catalyst for Carbon Dioxide Reforming of Methane: Ni/Ce-ZrO_2/θ-Al_2O_3. *Catal.* **2002**, *81*, 147–151.
79. Huang, X.J.; Mo, W.L.; He, X.Q.; Fan, X.; Ma, F.Y.; Tax, D. Effects of Promoters on the Structure, Performance, and Carbon Deposition of Ni-Al_2O_3 Catalysts for CO_2-CH_4 Reforming. *ACS Omega* **2021**, *6*, 16381–16390. [CrossRef]

80. Wang, N.; Yu, X.P.; Wang, Y.; Chu, W.; Liu, M. A comparison study on methane dry reforming with carbon dioxide over $LaNiO_3$ perovskite catalysts supported on mesoporous SBA-15, MCM-41 and silica carrier. *Catal. Today* **2013**, *212*, 98–107. [CrossRef]
81. Rashid, M.U.; Daud, W.M.A.W. Microemulsion based synthesis of Ni/MgO catalyst for dry reforming of methane. *RSC Adv.* **2016**, *6*, 38277–38289. [CrossRef]
82. Adans, Y.F.; Ballarini, A.D.; Martins, A.R.; Coelho, R.E.; Carvalho, L.S. Performance of nickel supported on gamma-Alumina obtained by aluminum recycling for methane dry reforming. *Catal. Lett.* **2017**, *147*, 2057–2066. [CrossRef]
83. Sun, J.W.; Wang, S.; Guo, Y.; Li, M.Z.; Zou, H.K.; Wang, Z.J. Carbon dioxide reforming of methane over nanostructured Ni/Al_2O_3 catalysts. *Catal. Commun.* **2018**, *104*, 53–56. [CrossRef]
84. Turap, Y.S.; Wang, I.W.; Fu, T.T.; Wu, Y.M.; Wang, Y.D.; Wang, W. Co-Ni alloy supported on CeO_2 as a bimetallic catalyst for dry reforming of methane. *Int. J. Hydrogen Energy* **2020**, *45*, 6538–6548. [CrossRef]
85. Huang, X.H.; Ji, Y.J.; Wei, T.; Jia, L.C.; Yan, D.; Li, J. High performance and stable mesoporous MgO-ZrO supported Ni catalysts for dry reforming of methane-ScienceDirect. *Curr. Res. Green Sustain. Chem.* **2021**, *4*, 100183. [CrossRef]
86. Ibrahim, A.A.; Fakeeha, A.H.; Abasaeed, A.E.; Al-Fatesh, A.S. Dry reforming of methane using Ni catalyst supported on ZrO_2, The effect of different sources of Zirconia. *Catalysts* **2021**, *11*, 827. [CrossRef]
87. Zhang, M.; Zhang, J.F.; Zhou, Z.L.; Zhang, Q.D.; Tan, Y.S.; Han, Y.Z. Effects of calcination atmosphere on the performance of the co-precipitated Ni/ZrO_2 catalyst in dry reforming of methane. *Can. J. Chem. Eng.* **2021**, *100*, 172–183.
88. Liu, D.P.; Quek, X.Y.; Cheo WN, E.; Lau, R.; Borgna, A.; Yang, Y. MCM-41 supported nickel-based bimetallic catalysts with superior stability during carbon dioxide reforming of methane: Effect of strong metal-support interaction. *J. Catal.* **2009**, *266*, 380–390. [CrossRef]
89. Bian, Z.F.; Das, S.; Wai, M.H.; Hongmanorom, P.; Kawi, S. A Review on Bimetallic Nickel-Based Catalysts for CO_2 Reforming of Methane. *ChemPhysChem* **2017**, *18*, 3117–3134. [CrossRef]
90. Mahboob, S.; Haghighi, M.; Rahmani, F. Sonochemically preparation and characterization of bimetallic $Ni-Co/Al_2O_3-ZrO_2$ nanocatalyst: Effects of ultrasound irradiation time and power on catalytic properties and activity in dry reforming of CH_4. *Ultrason. Sonochemistry* **2017**, *38*, 38–49. [CrossRef]
91. Dam, A.H.; Wang, H.M.; Niri, R.D.; Yu, X.F.; Walmsley, J.C.; Holmen, A.; Yang, J.; Chen, D. Methane Activation on Bimetallic Catalysts: Properties and Functions of Surface Ni-Ag Alloy. *ChemCatChem* **2019**, *11*, 3401–3412. [CrossRef]
92. Pawelec, B.; Damyanova, S.; Arishtirova, K.; Fierro, J.L.G.; Petrov, L. Structural and surface features of PtNi catalysts for reforming of methane with CO_2. *Appl. Catal. A Gen.* **2007**, *323*, 188–201. [CrossRef]
93. San-Jose-Alonso, D.; Juan-Juan, J.; Illan-Gomez, M.J.; Roman-Martinez, M.C. Ni, Co and bimetallic Ni-Co catalysts for the dry reforming of methane. *Appl. Catal. A Gen.* **2009**, *371*, 54–59. [CrossRef]
94. Wu, T.; Zhang, Q.; Cai, W.Y.; Zhang, P.; Song, X.F.; Sun, Z.; Cao, L. Phyllosilicate evolved hierarchical Ni-and Cu-Ni/SiO_2 nanocomposites for methane dry reforming catalysis. *Appl. Catal. A Gen.* **2015**, *503*, 94–102. [CrossRef]
95. Liu, H.L.; Nosheen, F.; Wang, X. Noble metal alloy complex nanostructures: Controllable synthesis and their electrochemical property. *Chem. Soc. Rev.* **2015**, *44*, 3056–3078. [CrossRef]
96. De, S.; Zhang, J.; Luque, R.; Yan, N. Ni-based bimetallic heterogeneous catalysts for energy and environmental applications. *Energy Environ. Sci.* **2016**, *9*, 3314–3347. [CrossRef]
97. Yu, X.P.; Zhang, F.B.; Wang, N.; Hao, S.X.; Chu, W. Plasma-Treated Bimetallic Ni-Pt Catalysts Derived from Hydrotalcites for the Carbon Dioxide Reforming of Methane. *Catal. Lett.* **2014**, *144*, 293–300. [CrossRef]
98. Hou, T.F.; Lei, Y.S.; Zhang, S.Y.; Zhang, J.H.; Cai, W.J. Ethanol dry reforming for syngas production over Ir/CeO_2 catalyst. *J. Rare Earths* **2015**, *33*, 42–45. [CrossRef]
99. Ma, Q.X.; Sun, J.; Gao, X.H.; Zhang, J.L.; Zhao, T.S.; Yoneyama, Y.; Tsubaki, N. Ordered mesoporous alumina-supported bimetallic Pd-Ni catalysts for methane dry reforming reaction. *Catal. Sci. Technol.* **2016**, *6*, 6542–6550. [CrossRef]
100. Oemar, U.; Hidajat, K.; Kawi, S. High catalytic stability of $Pd-Ni/Y_2O_3$ formed by interfacial Cl for oxy-CO_2 reforming of CH_4. *Catal. Today* **2017**, *281*, 276–294. [CrossRef]
101. Menning, C.A.; Chen, J.G. Thermodynamics and kinetics of oxygen-induced segregation of 3d metals in Pt-3d-Pt(111) and Pt-3d-Pt(100) bimetallic structures. *J. Chem. Phys.* **2008**, *128*, 164703. [CrossRef] [PubMed]
102. Menning, C.A.; Chen, J.G. General trend for adsorbate-induced segregation of subsurface metal atoms in bimetallic surfaces. *J. Chem. Phys.* **2009**, *130*, 174709. [CrossRef] [PubMed]
103. Garcia-Dieguez, M.; Pieta, I.S.; Herrera, M.C.; Larrubia, M.A.; Alemany, L.J. Nanostructured Pt- and Ni-based catalysts for CO_2-reforming of methane. *J. Catal.* **2010**, *270*, 136–145. [CrossRef]
104. Fan, M.S.; Abdullah, A.Z.; Bhatia, S. Utilization of greenhouse gases through carbon dioxide reforming of methane over $Ni-Co/MgO-ZrO_2$: Preparation, characterization and activity studies. *Appl. Catal. B Environ.* **2010**, *100*, 365–377. [CrossRef]
105. Qin, Z.Z.; Su, T.M.; Ji, H.B.; Jiang, Y.X.; Liu, R.W.; Chen, J.H. Experimental and theoretical study of the intrinsic kinetics for dimethyl ether synthesis from CO_2 over Cu-Fe-Zr/HZSM-5. *Aiche J.* **2015**, *61*, 1613–1627. [CrossRef]
106. Su, T.M.; Qin, Z.Z.; Ji, H.B.; Jiang, Y.X.; Huang, G. Recent advances in the photocatalytic reduction of carbon dioxide. *Environ. Chem. Lett.* **2016**, *14*, 99–112. [CrossRef]
107. Abukhadra, M.R.; Dardir, F.M.; Shaban, M.; Ahmed, E.A.; Soliman, M.F. Spongy Ni/Fe carbonate-fluorapatite catalyst for efficient conversion of cooking oil waste into biodiesel. *Environ. Chem. Lett.* **2017**, *16*, 665–670. [CrossRef]

108. Chen, L.; Huang, X.Y.; Tang, M.; Zhou, D.; Wu, F. Rapid dephosphorylation of glyphosate by Cu-catalyzed sulfite oxidation involving sulfate and hydroxyl radicals. *Environ. Chem. Lett.* **2018**, *16*, 1507–1511. [CrossRef]
109. Kumar, N.S.; Reddy, B.V.; Babu, M.S. Rapid synthesis of mono/bimetallic (Zn/Co/Zn-Co) zeolitic imidazolate frameworks at room temperature and evolution of their CO_2 uptake capacity. *Environ. Chem. Lett.* **2019**, *17*, 447–454.
110. Ray, K.; Sandupatla, A.S.; Deo, G. Activity and stability descriptors of Ni-based alloy catalysts for dry reforming of methane: A density functional theory study. *Int. J. Quantum Chem.* **2021**, *121*, e26580. [CrossRef]
111. Gonzalez-Delcruz, V.M.; Perenigue, R.; Ternero, F.; Holgado, J.P.; Caballero, A. In Situ XAS Study of Synergic Effects on Ni-Co/ZrO_2 Methane Reforming Catalysts. *J. Phys. Chem. C* **2012**, *116*, 2919–2926. [CrossRef]
112. Yu, M.; Zhu, K.; Liu, Z.; Xiao, H.; Deng, W.; Zhou, X. Carbon dioxide reforming of methane over promoted $Ni_xMg_{1-x}O(111)$ platelet catalyst derived from solvothermal synthesis. *Appl. Catal. B Environ.* **2014**, *148*, 177–190. [CrossRef]
113. Fan, X.; Liu, Z.; Zhu, Y.A.; Tong, G.S.; Zhang, J.D.; Engelbrekt, C.; Ulstrup, J.; Zhu, K.; Zhou, X.G. Tuning the composition of metastable $Co_xNi_yMg_{100-x-y}(OH)(OCH_3)$ nanoplates for optimizing robust methane dry reforming catalyst. *J. Catal.* **2015**, *330*, 106–119. [CrossRef]
114. Ay, H.; Uner, D. Dry reforming of methane over CeO_2 supported Ni, Co and Ni-Co catalysts. *Appl. Catal. B Environ.* **2015**, *179*, 128–138. [CrossRef]
115. Tsoukalou, A.; Imtiaz, Q.; Kim, S.M.; Abdala, P.M.; Yoon, S.; Muller, C.R. Dry-reforming of methane over bimetallic Ni-M/La_2O_3 (M=Co, Fe): The effect of the rate of $La_2O_2CO_3$ formation and phase stability on the catalytic activity and stability. *J. Catal.* **2016**, *343*, 208–214. [CrossRef]
116. Gao, X.Y.; Tan, Z.W.; Hidajat, K.; Kawi, S. Highly reactive Ni-Co/SiO_2 bimetallic catalyst via complexation with oleylamine/oleic acid organic pair for dry reforming of methane. *Catal. Today* **2017**, *281*, 250–258. [CrossRef]
117. Xu, L.L.; Wang, F.G.; Chen, M.; Fan, X.L.; Yang, H.M.; Nie, D.Y.; Qi, L. Alkaline-promoted Co-Ni bimetal ordered mesoporous catalysts with enhanced coke-resistant performance toward CO_2 reforming of CH_4. *J. CO2 Util.* **2017**, *18*, 1–14. [CrossRef]
118. Takanabe, K.; Nagaoka, K.; Nariai, K.; Aika, K. Influence of reduction temperature on the catalytic behavior of Co/TiO_2 catalysts for CO_2-CH_4 reforming and its relation with titania bulk crystal structure. *J. Catal.* **2005**, *230*, 75–85. [CrossRef]
119. Takanabe, K.; Nagaoka, K.; Nariai, K.; Aiak, K. Titania-supported cobalt and nickel bimetallic catalysts for carbon dioxide reforming of methane. *J. Catal.* **2005**, *232*, 268–275. [CrossRef]
120. Wu, Z.X.; Yang, B.; Miao, S.; Liu, W.; Xie, J.L.; Lee, S.; Pellin, M.J.; Xiao, D.Q.; Su, D.S.; Ma, D. Lattice strained Ni-Co alloy as high-performance catalyst for catalytic dry-reforming of methane. *ACS Catal.* **2019**, *9*, 2693–2700. [CrossRef]
121. Li, B.; Yuan, X.Q.; Li, L.Y.; Wang, X.J.; Li, B.T. Stabilizing Ni-Co alloy on bimodal mesoporous alumina to enhance carbon resistance for dry reforming of methane. *Ind. Eng. Chem. Res.* **2021**, *60*, 16874–16886. [CrossRef]
122. Liang, D.F.; Wang, Y.S.; Chen, M.Q.; Xie, X.L.; Li, C.; Wang, J.; Yuan, L. Dry reforming of methane for syngas production over attapulgite-derived MFI zeolite encapsulated bimetallic Ni-Co catalysts. *Appl. Catal. B Environ.* **2023**, *322*, 122088. [CrossRef]
123. Song, K.; Lu, M.M.; Xu, S.P.; Chen, C.Q.; Zhan, Y.Y.; Li, D.L.; Au, C.; Jiang, L.L.; Tomishige, K. Effect of alloy composition on catalytic performance and coke-resistance property of Ni-Cu/Mg(Al)O catalysts for dry reforming of methane. *Appl. Catal. B Environ.* **2018**, *239*, 324–333. [CrossRef]
124. Sagar, T.V.; Padmakar, D.; Lingaiah, N.; Prasad, P.S.S. Influence of Solid Solution Formation on the Activity of CeO_2 Supported Ni-Cu Mixed Oxide Catalysts in Dry Reforming of Methane. *Catal. Lett.* **2019**, *149*, 2597–2606. [CrossRef]
125. Wang, L.; Li, D.L.; Koike, M.; Watanabe, H.; Xu, Y.; Nakagawa, Y.; Tomishige, K. Catalytic performance and characterization of Ni-Co catalysts for the steam reforming of biomass tar to synthesis gas. *Fuel* **2013**, *112*, 654–661. [CrossRef]
126. Kim, S.M.; Abdala, P.M.; Margossian, T.; Hosseini, D.; Foppa, L.; Armutlulu, A.; Beek, W.V.; Comas-Vives, A.; Coperet, C.; Muller, C. Cooperativity and dynamics increase the performance of NiFe dry reforming catalysts. *J. Am. Chem. Soc.* **2017**, *139*, 1937–1949. [CrossRef]
127. Andraos, S.; Abbas-Ghaleb, R.; Chlala, D.; Vita, A.; Italiano, C.; Laganà, M.; Pino, L.; Nakhl, M.; Specchia, S. Production of hydrogen by methane dry reforming over ruthenium-nickel based catalysts deposited on Al_2O_3, $MgAl_2O_4$, and YSZ. *Int. J. Hydrogen Energy* **2019**, *44*, 25706–25716. [CrossRef]
128. Song, Z.; Wang, Q.; Guo, C.; Li, S.; Yan, W.; Jiao, W.; Qiu, L.; Yan, X.; Li, R. Improved effect of Fe on the stable NiFe/Al_2O_3 catalyst in low-temperature dry reforming of methane. *Ind. Eng. Chem. Res.* **2020**, *59*, 17250–17258. [CrossRef]
129. Chatla, A.; Ghouri, M.M.; El Hassan, O.W.; Mohamed, N.; Prakash, A.V.; Elbashir, N.O. An experimental and first principles DFT investigation on the effect of Cu addition to Ni/Al_2O_3 catalyst for the dry reforming of methane. *Appl. Catal. A* **2020**, *602*, 117699. [CrossRef]
130. Aghaali, M.H.; Firoozi, S. Enhancing the catalytic performance of Co substituted $NiAl_2O_4$ spinel by ultrasonic spray pyrolysis method for steam and dry reforming of methane. *Int. J. Hydrogen Energy* **2021**, *46*, 357–373. [CrossRef]
131. Hao, S.H.; Ma, F.Y.; Mo, W.L.; Li, M.F.; Zhu, W.J.; Zhang, J. Effect of additive La on the properties of CH_4/CO_2 reforming catalyst NiO/γ-Al_2O_3. *Nat. Gas Chem. Ind.* **2015**, *40*, 44–49.
132. Ruckenstein, E.; Hu, Y.H. Role of support in CO_2 reforming of CH_4 to syngas over Ni catalysts. *J. Catal.* **1996**, *162*, 230–238. [CrossRef]
133. Luisetto, I.; Tuti, S.; Romano, C.; Boaro, M.; Bartolomeo, E.D. Dry reforming of methane over Ni supported on doped CeO_2: New insight on the role of dopants for CO_2 activation. *J. CO2 Util.* **2019**, *30*, 63–78. [CrossRef]

134. Amin, M.H.; Sudarsanam, P.; Field, M.R.; Patel, J.; Bhargava, S.K. Effect of a Swelling Agent on the Performance of Ni/Porous Silica Catalyst for CH_4-CO_2 Reforming. *ACS Langmuir* **2017**, *33*, 10632–10644. [CrossRef]
135. Zhang, Q.L.; Zhang, T.F.; Shi, Y.Z.; Zhao, B.; Wang, M.Z.; Liu, Q.X.; Wang, J.; Long, K.X.; Duany, K.; Ning, P. A sintering and carbon-resistant Ni-SBA-15 catalyst prepared by solid-state grinding method for dry reforming of methane. *J. CO2 Util.* **2017**, *17*, 10–19. [CrossRef]
136. Tanggarnjanavalukul, C.; Donphai, W.; Witoon, T.; Chareonpanich, M.; Limtrakul, J. Deactivation of nickel catalysts in methane cracking reaction: Effect of bimodal mesomacropore structure of silica support. *Chem. Eng. J.* **2019**, *262*, 364–371. [CrossRef]
137. Du, X.J.; Zhang, D.S.; Shi, L.Y.; Gao, R.H.; Zhang, J.P. Coke- and sintering-resistant monolithic catalysts derived from in situ supported hydrotalcite-like films on Al wires for dry reforming of methane. *Nanoscale* **2013**, *5*, 2659–2663. [CrossRef]
138. Zhang, L.M.; Li, L.; Li, J.L.; Zhang, Y.H.; Hu, J.C. Carbon Dioxide Reforming of Methane over Nickel Catalyst Supported on MgO(111) Nanosheets. *Top. Catal.* **2014**, *57*, 619–626. [CrossRef]
139. Grigorkina, G.S.; Ramonova, A.G.; Kibizov, D.D.; Kozyrev, E.N.; Zaalishvili, V.B.; Fukutani, K.; Magkoev, T.T. Probing specific oxides as potential supports for metal/oxide model catalysts: MgO(111) polar film. *Solid State Commun.* **2017**, *257*, 16–19. [CrossRef]
140. Liu, S.G.; Guan, L.X.; Li, J.P.; Zhao, N.; Wei, W.; Sun, Y.H. CO_2 reforming of CH_4 over stabilized mesoporous Ni-CaO-ZrO_2 composites. *Fuel* **2008**, *87*, 2477–2481. [CrossRef]
141. Jafarbegloo, M.; Tarlani, A.; Mesbah, A.W.; Sahebdelfar, S. One-pot synthesis of NiO-MgO nanocatalysts for CO_2 reforming of methane: The influence of active metal content on catalytic performance. *J. Nat. Gas Sci. Eng.* **2015**, *27*, 1165–1173. [CrossRef]
142. Li, L.Z.; Yan, K.S.; Chen, J.; Feng, T.; Wang, F.M.; Wang, J.W.; Song, Z.L.; Ma, C.Y. Fe-rich biomass derived char for microwave-assisted methane reforming with carbon dioxide. *Sci. Total Environ.* **2019**, *657*, 1357–1367. [CrossRef] [PubMed]
143. Zhang, Z.H.; Ou, Z.L.; Qin, C.L.; Ran, J.Y.; Wu, C.F. Roles of alkali/alkaline earth metals in steam reforming of biomass tar for hydrogen production over perovskite supported Ni catalysts. *Fuel* **2019**, *257*, 116032. [CrossRef]
144. Li, L.; Yang, Z.; Chen, J.; Qin, X.; Jiang, X.; Wang, F.; Song, Z.; Ma, C. Performance of bio-char and energy analysis on CH_4 combined reforming by CO_2 and H_2O into syngas production with assistance of microwave. *Fuel* **2018**, *215*, 655–664. [CrossRef]
145. Jose-Alonso, D.S.; Illan-Gomez, M.J.; Roman-Martinez, M.C. K and Sr promoted Co alumina supported catalysts for the CO_2 reforming of methane. *Catal. Today* **2011**, *176*, 187–190. [CrossRef]
146. Wu, P.; Tao, Y.W.; Ling, H.J.; Chen, Z.B.; Ding, J.; Zeng, X.; Liao, X.Z.; Stampfl, C.; Huang, J. Cooperation of Ni and CaO at interface for CO_2 reforming of CH_4: A combined theoretical and experimental study. *ACS Catal.* **2019**, *9*, 10060–10069. [CrossRef]
147. Ruitenbeek, M.; Weckhuysen, B.M. A Radical twist to the versatile behavior of iron in selective methane activation. *Angew. Chem. International Ed.* **2014**, *53*, 11137–11139. [CrossRef]
148. Wang, J.; Mao, Y.R.; Zhang, L.Z.; Li, Y.L.; Liu, W.M.; Ma, Q.X.; Wu, D.S.; Peng, H.G. Remarkable basic-metal oxides promoted confinement catalysts for CO_2 reforming. *Fuel* **2022**, *315*, 123167. [CrossRef]
149. Kong, W.; Fu, Y.; Sun, Y.; Shi, L.; Li, S.G.; Vovk, E.; Zhou, X.H.; Si, R.; Pan, B.R.; Yuan, C.K.; et al. Nickel nanoparticles with interfacial confinement mimic noble metal catalyst in methane dry reforming. *Appl. Catal. B Environ.* **2021**, *285*, 119837. [CrossRef]
150. Zhang, L.; Lian, J.; Li, L.; Peng, C.; Liu, W.M.; Xu, X.L.; Fang, X.Z.; Wang, Z.; Wang, X.; Peng, H.E. $LaNiO_3$ nanocube embedded in mesoporous silica for dry reforming of methane with enhanced coking resistance. *Microporous Mesoporous Mater.* **2018**, *266*, 189–197. [CrossRef]
151. Liu, W.M.; Li, L.; Lin, S.X.; Luo, Y.W.; Bao, Z.H.; Mao, Y.R.; Li, K.Z.; Wu, D.S.; Peng, H.G. Confined Ni-In intermetallic alloy nanocatalyst with excellent coking resistance for methane dry reforming. *J. Energy Chem.* **2022**, *65*, 34–47. [CrossRef]
152. Wang, L.H.; Hu, R.; Liu, H.; Wei, Q.H.; Gong, D.D.; Mo, L.Y.; Tao, H.C.; Zhuang, Z.H. Encapsulated Ni@La_2O_3/SiO_2 catalyst with a one-pot method for the dry reforming of methane. *Catalysts* **2020**, *10*, 38. [CrossRef]
153. Nematollahi, B.; Rezaei, M.; Lay, E.N.; Khajenoori, M. Thermodynamic analysis of combined reforming process using Gibbs energy minimization method: In view of solid carbon formation. *J. Nat. Gas Chem.* **2012**, *21*, 694–702. [CrossRef]
154. Jang, W.J.; Jeong, D.W.; Shim, J.O.; Kim, H.M.; Roh, H.S.; Son, I.H.; Lee, S.J. Combined steam and carbon dioxide reforming of methane and side reactions: Thermodynamic equilibrium analysis and experimental application. *Appl. Energy* **2016**, *173*, 80–91. [CrossRef]
155. Nikoo, M.K.; Amin, N.A.S. Thermodynamic analysis of carbon dioxide reforming of methane in view of solid carbon formation. *Fuel Process. Technol.* **2011**, *92*, 678–691. [CrossRef]
156. Bao, Z.H.; Lu, Y.W.; Han, J.; Li, Y.B.; Yu, F. Highly active and stable Ni-based bimodal pore catalyst for dry reforming of methane. *Appl. Catal. A Gen.* **2015**, *491*, 116–126. [CrossRef]
157. Li, C.L.; Fu, Y.L.; Meng, M.; Bian, G.Z.; Xie, Y.N.; Hu, T.D.; Zhang, J. EXAFS study on the effect of water vapor addition on the structure of Ni components in the CH_4-CO_2 reforming catalyst Ni/CeO_2-ZrO_2-Al_2O_3. *Nucl. Tech.* **2002**, *(10)*, 879–882.
158. O'Connor, A.M.; Ross, J.R.H. The effect of O_2 addition on the carbon dioxide reforming of methane over Pt/ZrO_2 catalysts. *Catal. Today* **1998**, *46*, 203–210. [CrossRef]
159. Li, L.Z.; Jiang, X.W.; Wang, H.G.; Song, Z.L.; Ma, C.Y. Combined reforming of CH_4 with CO_2/steam assisted by microwave. *Combust. Sci. Technol.* **2017**, *23*, 293–298.